Potential Artifacts of Sequential State Estimation: Invariants

Carl Wunsch*
Department of Earth and Planetary Sciences
Harvard University
Cambridge MA 02138
email: cwunsch@fas.harvard.edu

September 7, 2021

Abstract

In sequential estimation methods often used in general climate or oceanic calculations of the state and of forecasts, *observations act mathematically and statistically as forcings* as is obvious in the innovation form of the equations. For purposes of calculating changes in important functions of state variables such as total mass and energy, or in volumetric current transports, results are sensitive to mis-representation of a large variety of parameters including initial conditions, various uncertainty covariances, and systematic and random errors in observations. Errors can be both stochastic and systematic, with the latter, as usual, being the most intractable. Here, in Part 1, some of the consequences of such errors are analyzed in the context of a simplified mass-spring oscillator system exhibiting many of the issues of far more complicated realistic problems. Part 2 applies the same methods to a slightly more geophysical barotropic Rossby wave plus western boundary current system. The overall message is that convincing trend and other time-dependent determinations in "reanalyis" like estimates requires a full understanding of *both* models and observations.

Part 1. Formalism and Simplified System

1 Introduction

Intense scientific and practical interest exists in understanding the time-dependent behavior in the past and future of elements of the climate system. Best estimates of past, present, and future

*Also, Dept. of Earth, Atmospheric and Planetary Sciences, MIT

invoke knowledge of both observations and models. These both can involve physical-dynamical, chemical, and biological elements.

Fundamental to understanding many physical systems is analysis of long-term changes in quantities such as energy, enstrophy, total mass, mean concentrations, that are subject to various conservation rules. These elements, absent external perturbations or internal sources or sinks, can be usefully regarded as potential "invariants" of the system[1]. In conventional science, violation e.g., of mass or energy conservation not attributable to specific disturbances, would preclude any claim to understanding of the physics, chemistry, etc. governing the temporal evolution. Observational scientific fields in which time series data are of basic importance thus struggle with inferences from changing observation systems—either or both of changing technology or of spatial and temporal distributions. In climate science particularly, both of these factors determine the ability to determine trends over months, decades and longer.

In addition, much interest exists in the possibility of trends in major sub-elements of the system—oceanographically for example, in the transports of mass or heat or other properties in major currents such as the Gulf Stream. "Best estimates" of these values are also made using combinations of kinematic and dynamical models plus observations.

Methods for combining data with models fall into the general category of control theory, although full understanding is made difficult by the need to combine major sub-elements of different disciplines, including statistics of several types, computer science, numerical approximations, oceanography, meteorology, climate, dynamical systems theory, and the observational characteristics of very diverse instrument types and distributions. Within the control theory context, distinct goals include "filtering" (what is the present system state?), "prediction" (what is the best estimate of the future state?), and "interval smoothing" (what was the time history over some finite past interval?) and their corresponding uncertainties. In the climate context, a great deal of effort has been directed toward using the machinery of numerical weather forecasting, usually labelled as "reanalysis," for all three of these goals, often without distinguishing the purposes.

One example, of intense interest, is the skill with which one can detect trends in climate-related variables in the presence of both model and data errors occurring over many past decades and longer. Particular attention is called to the paper of Bengtsson et al. (2004) who showed the impacts of observational system shifts on outcomes with some sequential methods. A number of subsequent papers (e.g., Bromwich and Fogt, 2004; Bengtsson et al., 2007; Carton and Giese, 2008; Thorne and Vose, 2010) have called attention to difficulties in using "reanalyses" for long-

[1]The modifier "potential" is normally omitted here, being implicit as requiring the absence of generalized dissipation and external forces.

term climate properties sometimes ending with advice—such as "minimize the errors" (and see Wunsch, 2020 for one global application).

For some purposes e.g., short-term weather or other prediction, system failure to conserve mass or energy or enstrophy may be of no concern—as the time-scale for measurable consequence of that failure to emerge can greatly exceed the forecast time. In contrast, for reconstruction of past states for trend determination, those consequences can destroy any hope of physical interpretation. In long-duration forecasts with rigorous models, but by definition, no observational data at all, invariants are likely to be preserved, albeit tests of model elements and in particular of accumulating errors, are not possible.

What can go astray? This analysis is intended as an analogue of the way in which greatly simplified geophysical fluid dynamics models are used to understand much more realistic systems. It might be thought of as "geophysical fluid statistics (GFS)", as distinct e.g., from full statistical theories of turbulence. Analyzing very simple systems with order tens of unknowns should help understanding of those with $N \rightarrow 10^{10}+$ unknowns without making any claim to necessarily being able to scale up the results to full climate system dimensions. To keep the focus on the physical results, most of the necessary algebra is here consigned for reference to a series of Appendices and to cited standard textbook coverage. What follows has a faintly pedagogical air—justified perhaps by the now somewhat notorious, contradictory, results in the public domain (e.g., Hu et al., 2020; Boers, 2021) and the wide impression that "reanalysis" methods are not well understood in the wider community,

2 Some Concepts and Notation

Models

Some basic notation is necessary to analyze even the simplest, linear, time-evolving system with data. A fuller account is given in Appendix A (or see Wunsch, 2006, hereafter W06, or many other textbook references. Notation here is similar to that in W06.). Let $\mathbf{x}(t)$ be a state vector in discrete time $t = 0, \Delta t, ..., M_t \Delta t = t_f$. A "state vector" is one that completely describes a linear physical system evolving according to a *perfect* model rule,

$$\mathbf{x}(t + \Delta t, -) = \mathbf{A}(t)\,\mathbf{x}(t, -) + \mathbf{B}(t)\,\mathbf{q}(t), \tag{1}$$ {perfmodel}

where $\mathbf{A}(t)$ is the "state transition matrix". $\mathbf{B}(t)\,\mathbf{q}(t)$ is a very general representation of boundary conditions and any internal sources or sinks in which $\mathbf{B}(t)$ simply distributes the time-evolving field, $\mathbf{q}(t)$, amongst state vector elements. $\Delta t > 0$ is a fixed time-step. A minus sign has been entered into the argument—from a control theory convention—to indicate that no data are being used.

Such perfect models do not exist in practice and the system is usefully rewritten as,

$$\tilde{\mathbf{x}}(t+\Delta t,-)=\mathbf{A}(t)\,\tilde{\mathbf{x}}(t,-)+\mathbf{B}(t)\,\mathbf{q}(t)+\mathbf{\Gamma}(t)\,\mathbf{u}(t)\,. \tag{2}$$ {linmodel1}

A tilde, ˜, indicates that the solutions to Eq. (2) are at best an approximation to or estimate of the true state vector. $\Gamma(t)\,\mathbf{u}(t)$, a flexible structure is introduced as the *unknown* elements and corrections to $\mathbf{B}(t)\,\mathbf{q}(t)$ for boundary/initial conditions, internal parameterizations, and forcing generally. Eq. (2) will be referred to below as the "prediction model," as it is used in practice to make the best prediction at any future time—given the immediate past best-estimate. In such a calculation, $\mathbf{u}(t)=0$, as it is otherwise unknown. In many circumstances (e.g., Brown and Hwang, 1997, W06), Eqs. (1 or 2) are linearized about some reference state. That $\mathbf{A}(t)$ is itself then, and always, subject to significant error is a very important point, but that possibility renders the problem non-linear, and for present purposes the implications and approaches are set aside.

Time-evolving systems require initial conditions, $\tilde{\mathbf{x}}(0)$, having some known or assumed error (uncertainty), written for linear systems as a covariance matrix,

$$\mathbf{P}(0)=\left\langle[\tilde{\mathbf{x}}(0)-\mathbf{x}(0)]\,[\tilde{\mathbf{x}}(0)-\mathbf{x}(0)]^{T}\right\rangle \tag{3}$$

and with the further, sometimes wholly implicit, assumption that the mean error $\langle\tilde{\mathbf{x}}(0)-\mathbf{x}(0)\rangle=\mathbf{0}$. The brackets denote an expected value, whether theoretical or estimated. Uncertainties generally determine the utility of any solution of any problem. Part of the estimation problem is to cope with the possibility that $\mathbf{P}(0)$ itself is not wholly accurate, and with implications depending on how long the system "remembers" its initial conditions (typically a function of $\mathbf{A}$).

Data

Suppose now that at time $t=\tau>0$ some data are available, written generally, but linearly, as,

$$\mathbf{y}(\tau)=\mathbf{E}(\tau)\,\mathbf{x}(\tau)+\mathbf{n}(\tau)\,, \tag{4}$$ {data2}

where $\mathbf{n}(\tau)$ is usually *assumed* to be a zero-mean unimodally distributed noise process in the observations, with known covariance matrix, $\mathbf{R}(\tau)$, and which is often time-dependent and often again assumed to be diagonal. (Non-linear observations, for example that of a speed, require special treatment.) Observation matrix $\mathbf{E}(\tau)$ appropriately distributes the elements of $\mathbf{x}(\tau)$ making up the observations, and which can range from observation of a single element, $x_j(\tau)$, to some arbitrarily complicated linear combination of different elements (e.g., weighted averages or differences).

Formally, one can deduce another estimate of $\mathbf{x}(\tau)$ directly from Eq. (4) as,

$$\tilde{\mathbf{x}}(\tau, y) = \mathbf{E}(\tau)^{+} \mathbf{y}(\tau) \pm \mathbf{n}_E(\tau), \tag{5a}$$ {staticinv}

$$\mathbf{P}_E(\tau) = \left\langle [\tilde{\mathbf{x}}(\tau, y) - \mathbf{x}(\tau)] [\tilde{\mathbf{x}}(\tau, y) - \mathbf{x}(\tau)]^T \right\rangle, \tag{5b}$$

where $\mathbf{E}(\tau)^{+}$ is a generalized inverse deduced from standard, static, linear inverse methods using appropriate row and column scaling, and would be accompanied by an uncertainty $\mathbf{P}_E(\tau)$ and a resolution analysis. Such static, fixed-time, calculations for time-dependent systems are uncommon, as $\mathbf{E}(\tau)^{+}$ usually has a vast unknown nullspace in $\mathbf{P}_E(\tau)$, dependent upon how comprehensive and accurate the data are.

Combining Data and Models

Suppose, as is commonplace in numerical weather prediction and in reanalyses, that the prediction model is used to forecast the state at time τ, written as $\tilde{\mathbf{x}}(\tau, -)$. Given the initial condition error $\mathbf{P}(0)$, a straightforward calculation (see Appendix A) produces an expected error of the forecast,

$$\mathbf{P}(\tau, -) = \left\langle [\tilde{\mathbf{x}}(\tau, -) - \mathbf{x}(\tau)] [\tilde{\mathbf{x}}(\tau, -) - \mathbf{x}(\tau)]^T \right\rangle.$$

If data also exist at time τ, then a linear inversion, if carried out as in Eq. (5a), provides another estimate of the state, with its own uncertainty, dependent upon $\mathbf{R}(\tau)$ and the structure of $\mathbf{E}(\tau)$. Evidently, a better estimate than either is to combine them, inversely proportional to their uncertainties, as is conventional in recursive least-squares, resulting in,

$$\tilde{\mathbf{x}}(\tau) = \tilde{\mathbf{x}}(\tau, -) + \mathbf{K}(\tau) [\mathbf{y}(\tau) - \mathbf{E}(\tau) \tilde{\mathbf{x}}(\tau, -)]. \tag{6}$$ {kf1}

The "gain" matrix is,

$$\mathbf{K}(\tau) = \mathbf{P}(\tau, -) \mathbf{E}(\tau)^T \left[\mathbf{E}(\tau) \mathbf{P}(\tau, -) \mathbf{E}(\tau)^T + \mathbf{R}(\tau) \right]^{-1}. \tag{7}$$ {gain1}

In this form, $\mathbf{K}$ is the "Kalman gain" and the operation is the "Kalman filter" and which includes, for discrete time, the uncertainty of the combined estimate,

$$\begin{aligned} \mathbf{P}(\tau) &= \mathbf{P}(\tau, -) - \mathbf{K}(\tau) \mathbf{E}(\tau) \mathbf{P}(\tau, -) \\ &= \mathbf{P}(\tau, -) - \mathbf{P}(\tau, -) \mathbf{E}(\tau)^T \left[\mathbf{E}(\tau) \mathbf{P}(\tau, -) \mathbf{E}(\tau)^T + \mathbf{R}(\tau) \right]^{-1} \mathbf{E}(\tau) \mathbf{P}(\tau, -), \end{aligned} \tag{8}$$ {poftau}

a matrix Riccati equation which is again a result of recursive least-squares.[2] Textbooks prove that the norm, $\|\mathbf{P}(\tau)\| \leq \|\mathbf{P}(\tau, -)\|$, that is, if used realistically, the data cannot worsen the error in the forecast, but can potentially improve it, perhaps greatly, depending upon $\mathbf{E}(\tau), \mathbf{R}(\tau)$. (A tilde can sensibly be placed on $\mathbf{P}, \mathbf{R}$, but is omitted here.)

[2] The history of the Kalman filter dates to the 19th Century. See Lauritzen, 1981.

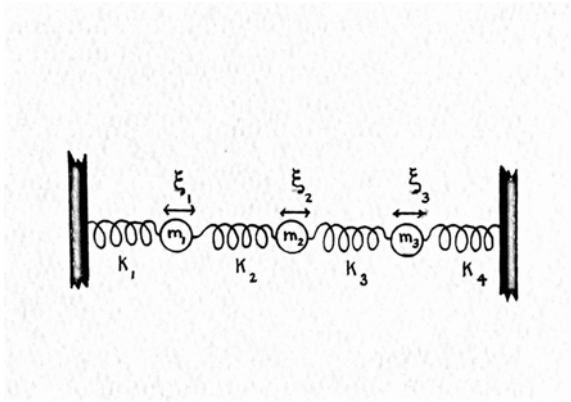

Figure 1: Mass-spring oscillator system used as a detailed example. Although the sketch is slightly more general, here all masses have the same value, m, and all spring constants and Rayleigh dissipation coefficients k, r are the same. {mass_spring_s

Innovation Forms

A slight modification of the system is to combine Eqs. (2) and (6) into the "innovation" forms,

$$\tilde{\mathbf{x}}(t+\Delta t) = \mathbf{A}(t)\,\tilde{\mathbf{x}}(t,-) + \mathbf{B}(t)\,\mathbf{q}(t) + \mathbf{K}(t)\left[\mathbf{y}(t) - \mathbf{E}(t)\,\mathbf{x}(t)\right], \tag{9}$$ {innov1}

again setting the unknown $\mathbf{\Gamma}(t)\,\mathbf{u}(t) = 0$, or,

$$\begin{aligned} \tilde{\mathbf{x}}(t+\Delta t) &= \mathbf{A}_1(t)\,\tilde{\mathbf{x}}(t,-) + \mathbf{B}(t)\,\mathbf{q}(t) + \mathbf{K}(t)\,\mathbf{y}(t), \\ \mathbf{A}_1(t) &= \mathbf{A}(t) - \mathbf{K}(t)\,\mathbf{E}(t), \end{aligned} \tag{10}$$ {innov2}

(Goodwin and Sin, 1984, P. 251), whose importance is that both show explicitly that *data introduction acts as an analogue of externally imposed forcing.*

3 Simple Example: Mass-Spring Oscillator

For a simple, intuitively accessible analogue system, consider the mass-spring oscillator, following McCuskey, 1959, Goldstein, 1980, W06, Strang, 2007) in the conventional continuous time formulation of simultaneous differential equations. Three identical masses, $m = 1$, are connected to each other and to a wall at either end by springs of identical constant, k (Fig. 1). Movement is damped by a Rayleigh friction coefficient, r. Generalization to differing- masses, spring constants, and dissipation coefficients is straightforward. Displacements of each mass are $\xi_i(t)$,

$i = 1, 2, 3$. The linear Newtonian equations of coupled motion are, {xieqs1}

$$m\frac{d^2\xi_1}{dt^2} + k\xi_1 + k\left(\xi_1 - \xi_2\right) + r\frac{d\xi_1}{dt} = q_{c1}\left(t\right) \tag{11a}$$

$$m\frac{d^2\xi_2}{dt^2} + k\xi_2 + k\left(\xi_2 - \xi_1\right) + k\left(\xi_2 - \xi_3\right) + r\frac{d\xi_2}{dt} = q_{c2}\left(t\right) \tag{11b}$$

$$m\frac{d^2\xi_3}{dt^2} + k\xi_3 + k\left(\xi_3 - \xi_2\right) + r\frac{d\xi_3}{dt} = q_{c3}\left(t\right). \tag{11c}$$

This second-order system is reduced to a canonical form of coupled first-order equations by introduction of a continuous time state vector, the column vector,

$$\mathbf{x}_c\left(t\right) = \left[\xi_1\left(t\right), \xi_2\left(t\right), \xi_3\left(t\right), d\xi_1/dt, d\xi_2/dt, d\xi_3/dt\right]^T, \tag{12}$$

where superscript T denotes the transpose. Note the mixture of dimensional units in the elements of $\mathbf{x}_c\left(t\right)$, identifiable with the Hamiltonian variables of position and momentum. $d\xi_i/dt$ is sometimes written $\dot{\xi}_i$. Then Eqs. (11) become (setting $m = 1$, or dividing through by it),

$$\frac{d\mathbf{x}_c\left(t\right)}{dt} = \mathbf{A}_c\mathbf{x}_c\left(t\right) + \mathbf{B}_c\mathbf{q}_c\left(t\right), \tag{13}$$ {canon0}

where

$$\mathbf{A}_c = \left\{\begin{array}{cccccc} 0 & 0 & 0 & 1 & 0 & 0 \\ -0 & 0 & 0 & 0 & 1 & 0 \\ 0 & 0 & 0 & 0 & 0 & 1 \\ -2k & k & 0 & -r & 0 & 0 \\ k & -2k & k & 0 & -r & 0 \\ 0 & k & -2k & 0 & 0 & -r \end{array}\right\} = \left\{\begin{array}{cc} \mathbf{0}_3 & \mathbf{I}_3 \\ \mathbf{K}_c & \mathbf{R}_c \end{array}\right\}, \tag{14}$$ {ac1}

defining the 3x3 block matrices, $\mathbf{K}_c, \mathbf{R}_c$ symmetric and diagonal respectively, and are constant. $\mathbf{B}_c$ distributes inputs, $\mathbf{q}_c = \left[q_{c1}, q_{c2}, ..., q_{c6}\right]^T$, variously amongst the six sub-equations. Putting e.g., $r = 0.5, k = 30$, $\mathbf{A}$ is full-rank with 3 pairs of complex conjugate eigenvalues, but non-orthonormal right eigenvectors. These parameter values are generally used throughout. Here, and in what follows, the system is notationally simplified by using time-constant $\mathbf{A}, \mathbf{B}$.

Textbooks (e.g., Bellman, 1960; Brogan, 1991; Anderson and Moore, 1979) show that Eq. (42) is a very general form for any linear system. For constant $\mathbf{A}_c, \mathbf{B}_c$, Eq. (42) is readily solved analytically as,

$$\mathbf{x}_c\left(t\right) = e^{\mathbf{A}_c t}\mathbf{x}_c\left(0\right) + \int_0^t e^{\mathbf{A}_c \tau}\mathbf{B}_c\mathbf{q}_c\left(\tau\right)d\tau, \tag{15}$$

where $\mathbf{x}_c\left(0\right)$ are the required initial conditions at $t = 0$. The physics of such small oscillations is discussed in most classical mechanics textbooks and is omitted here.

Energy

Consider now an energy principle. Define a reduced state vector,

$$\mathbf{x}_{red} = \left\{ \begin{array}{cc} \mathbf{0}_3 & \mathbf{0}_3 \\ \mathbf{0}_3 & \mathbf{I}_3 \end{array} \right\} \mathbf{x}_c(t) = \mathbf{F} \left[\begin{array}{c} \boldsymbol{\xi} \\ d\boldsymbol{\xi}/dt \end{array} \right] = \left[\begin{array}{c} \mathbf{o}_3 \\ d\boldsymbol{\xi}(t)/dt \end{array} \right], \tag{16}$$

containing only the velocity components. Define, without dissipation ($\mathbf{R}_c = \mathbf{0}$),

$$\mathcal{E}_c(t) = \frac{1}{2} \left[\left(\frac{d\boldsymbol{\xi}}{dt} \right)^T \left(\frac{d\boldsymbol{\xi}}{dt} \right) - \boldsymbol{\xi}^T \mathbf{K}_c \boldsymbol{\xi} \right] \tag{17}$$ {ec}

$$\frac{d\mathcal{E}_c(t)}{dt} = -\mathbf{x}_c(t)^T \mathbf{F}^T \mathbf{A}_c \mathbf{x}_c(t) = \frac{1}{2} \frac{d}{dt} \left[\left(\frac{d\boldsymbol{\xi}}{dt} \right)^T \left(\frac{d\boldsymbol{\xi}}{dt} \right) - \boldsymbol{\xi}^T \mathbf{K}_c \boldsymbol{\xi} \right] \tag{18}$$ {econdiss}

the sum of the kinetic and potential energies (the minus sign compensates for the negative definitions in $\mathbf{K}_c$) and is here a Hamiltonian. The non-diagonal elements of $\mathbf{K}_c$ redistribute the potential energy amongst the masses through time.

With finite dissipation and forcing, from Eq. (42),

$$\frac{d\mathcal{E}_c(t)}{dt} = \left(\frac{d\boldsymbol{\xi}}{dt} \right)^T \mathbf{R}_c \left(\frac{d\boldsymbol{\xi}}{dt} \right) + \frac{d\boldsymbol{\xi}}{dt}^T \mathbf{B}_c \mathbf{q}(t). \tag{19}$$ {diff_energy_t

$d\mathcal{E}_c(t)/dt = 0$, if the forcing and dissipation vanish.

An interesting general question is whether, for arbitrary square $\mathbf{A}_c$, an $\mathbf{F}$ can be found such that there is a quadratic invariant equivalent to $\mathcal{E}_c$? An approach using symplectic methods appears feasible, but is not pursued here. See also Hill and Moylan (1980), Tan et al. (1999).

Discrete Version

Write Eq. (1) at constant, discrete, time intervals, Δt, using an Eulerian time-step in the same form,

$$\mathbf{x}(t + \Delta t) = \mathbf{A}\mathbf{x}(t) + \mathbf{B}\mathbf{q}(t), t = m\Delta t, m = 0, 1, 2, ... \tag{20}$$ {canondisc}

$$\mathbf{A} = \mathbf{I}_6 + dt\mathbf{A}_c, \tag{21}$$

and the prediction model is unchanged except now,

$$\mathbf{A} = \left\{ \begin{array}{cccccc} 1 & 0 & 0 & \Delta t & 0 & 0 \\ -0 & 1 & 0 & 0 & \Delta t & 0 \\ 0 & 0 & 1 & 0 & 0 & \Delta t \\ -2k\Delta t & k\Delta t & 0 & (1-r)\Delta t & 0 & 0 \\ k\Delta t & -2k\Delta t & k\Delta t & 0 & (1-r)\Delta t & 0 \\ 0 & k\Delta t & -2k\Delta t & 0 & 0 & (1-r)\Delta t \end{array} \right\} \tag{22}$$ {Adisc}

$$= \left\{ \begin{array}{cc} \mathbf{I}_3 & \Delta t\mathbf{I}_3 \\ \Delta t\mathbf{K}_c & \mathbf{I}_3 + \Delta t\mathbf{R}_c \end{array} \right\} \tag{23}$$

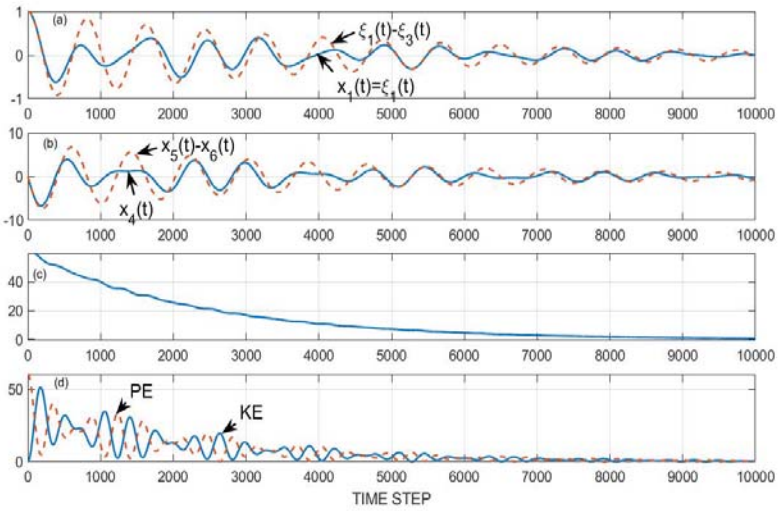

Figure 2: The unforced case, initial condition vanishing except for $x_1(t) = 1$. Natural frequency and decay scale are apparent. (a) $x_1(t) = \xi_1(t)$ (solid) and $\xi_1(t) - \xi_2(3)$(dashed). (b) $d\xi_4/dt = \dot{\xi}_4$ and $\dot{\xi}_4 - \dot{\xi}_6$ (dashed). (c) $\mathcal{E}(t)$ showing decay scale from the initial displacement. (d) Kinetic energy (solid) and potential energy making up $\mathcal{E}(t)$

{osc_initcondo

An example for the nearly dissipationless, unforced, example of the oscillator solution, from the discrete formulation is shown in Fig. 2 for elements of $x_i(t)$. Non-zero values here arise only from the initial conditions, $\mathbf{x}(0) = [1, 0, 0, ...]^T$. A small amount of dissipation was included to stabilize the particularly simple numerical scheme. From the particular choice of the discrete state vector, the energy, (Fig. 2), is formally identical to that in the continuous case,

$$\frac{\mathcal{E}_c(t) - \mathcal{E}_c(t - \Delta t)}{\Delta t} = \left(\frac{d\boldsymbol{\xi}}{dt}\right)^T \mathbf{R}_c \left(\frac{d\boldsymbol{\xi}}{dt}\right) + \frac{d\boldsymbol{\xi}}{dt}^T \mathbf{B}_c \mathbf{q}(t). \tag{24}$$

$\mathcal{E}_c(t)$ and the potential and kinetic energies through time are also shown. The basic oscillatory nature of the state vector elements is plain, and the decay time is also visible.

The total energy declines by about 2% in an initial transient and then stabilizes with small numerical oscillations at about 5000 time steps. Kinetic energy is oscillatory as energy is exchanged with the potential component.

4 Mass-Spring Oscillator with Observations

If the innovation form of the evolution Eq. (9) is used, the energy change becomes, numerically, accounting for the observations,

$$\frac{\mathcal{E}_c(t) - \mathcal{E}_c(t-\Delta t)}{\Delta t} \approx \left(\frac{d\boldsymbol{\xi}}{dt}\right)^T \mathbf{R}_c \left(\frac{d\boldsymbol{\xi}}{dt}\right) + \frac{d\boldsymbol{\xi}}{dt}^T \mathbf{B}_c \mathbf{q}(t) + \frac{d\mathbf{x}(t)}{dt}^T \mathbf{K}(t)\left[\mathbf{y}(t) - \mathbf{E}(t)\,\mathbf{x}(t)\right] \quad (25)$$

{Einnov}

showing explicitly the influence of the observations on the computed energy. With intermittent observations and/or with changing structures, $\mathbf{E}(t)$, then $\mathcal{E}_c(t)$ will undergo forced abrupt changes—as expected.

Given the very large number of potentially erroneous elements in any choice of model and data and data distributions, and the ways in which they interact when integrated through time, a comprehensive discussion even of the 6-element state vector mass-spring oscillator system is difficult. Instead, some simple examples exploring primarily the influence of data density on the state estimate and of its mechanical energy are described. One can experiment with the model and its time-constants, model time-step, accuracies and corresponding covariances of initial conditions, boundary conditions, data etc. The basic problems of any linear system already emerge in this simple example.

Consider, using the same k, r, $\Delta t = .001$ to represent "truth" where the forcing $\mathbf{Bq}(t) = q_1(t) = 0.1\cos(2\pi t/(2.5T_{diss})) + \varepsilon(t)$, that is, only mass 1 is forced in position, and with a low frequency not equal to one of the natural frequencies. $T_{diss} = 1/r$, is the dissipation time. $\varepsilon(t)$ is a white noise element. Initial condition is $\xi_1(0) = 1$, all other elements vanishing; see Fig. 3. Accumulation of the influence of the stochastic element in the forcing clearly depends upon details of the model time-scales and if $\varepsilon(t)$ were not white noise, on its spectrum as well. In all cases, the cumulative effect of a random forcing will have the nature of a random walk—with details dependent upon the forcing structure, as well as the memory elements of the model time scales.

The prediction model (Fig. 5a) has correct initial conditions and $\mathbf{A}, \mathbf{B}$ matrices, but is forced by the deterministic component with 1/2 the correct amplitude, and with the stochastic component being treated as fully unknown—replaced by its zero mean The added noise in the measurements has a standard deviation of 0.2 of the total forcing, the latter standard deviation including that of the deterministic contribution.

Near-Perfect Observations: Two Times and Multiple Times

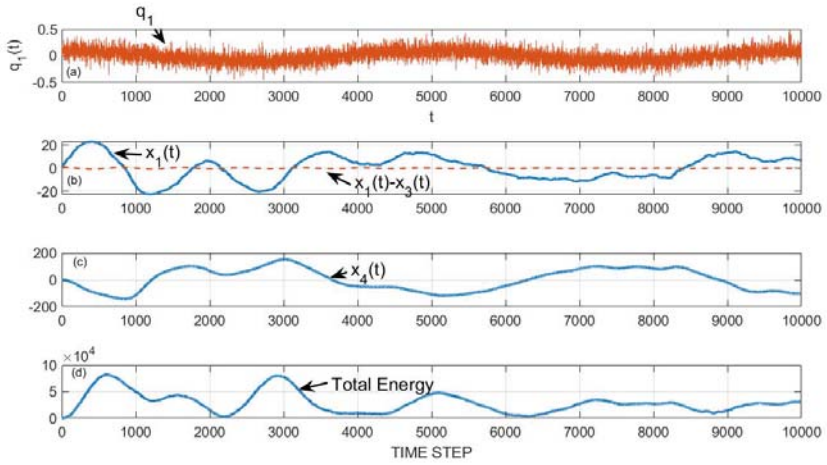

Figure 3: Forced version of the same oscillator system as in Fig. 2. Forcing is a low-frequency periodic sinusoid plus a pure white noise disturbance at every time-step in mass 1 position alone. (a) The forcing, q_1, white noise plus the visible low frequency sinusoid; (b) $x_1(t) = \xi_1(t), x_1(t) - x_3(t)$; (c) $x_4(t) = dx_1/dt = \dot{\xi}_1(t)$. (d) Total energy through time, $\mathcal{E}(t)$. Energy varies with the random walk arising from $\varepsilon(t)$ as well as from the deterministic forcing.

{osc_forced_pe

To demonstrate the most basic problem of energy, consider a nearly-perfect observation of all 6 positions at two times$\tau_{1,2}$ as displayed in Fig. 4 with $\mathbf{E} = \mathbf{I}_6$ No observational null-space exists. Although the new estimate of the state vector is an improvement over that from the pure forecast, any effort to calculate a trend in energy of the system will fail unless very careful attention is paid to correcting for the invariant violation at the time of the observation. Fig. 5 shows the results when observations occur in clusters having different intervals between the measurements. Visually, the displacement and energy have a periodicity imposed by the observation time-intervals and readily confirmed by fourier analysis.

Quadratic Variability

In a linear system, a Gaussian assumption for the dependent variables is commonly appropriate. By focussing here on the quadratic invariant of energy, the variables become χ^2 distributed. Thus the $\xi_i^2, \dot{\xi}_i^2$ have such distributions, but with differing means and variances, and with potentially very strong correlations, so that they cannot be regarded as independent variables. Determining the uncertainties of the six uncertain covarying elements making up $\mathcal{E}(t)$ involves some intricacy. A formal analysis can be made of the resulting probability distribution for the sum in $\mathcal{E}(t)$, involving non-central χ^2 distributions (Imhof, 1961, Sheil and O'Muircheartaigh, 1977, Davies, 1980). In view of the purpose and simplicity of this example however, an estimate of the uncertainty was made by simply generating 50 different versions of the observations,

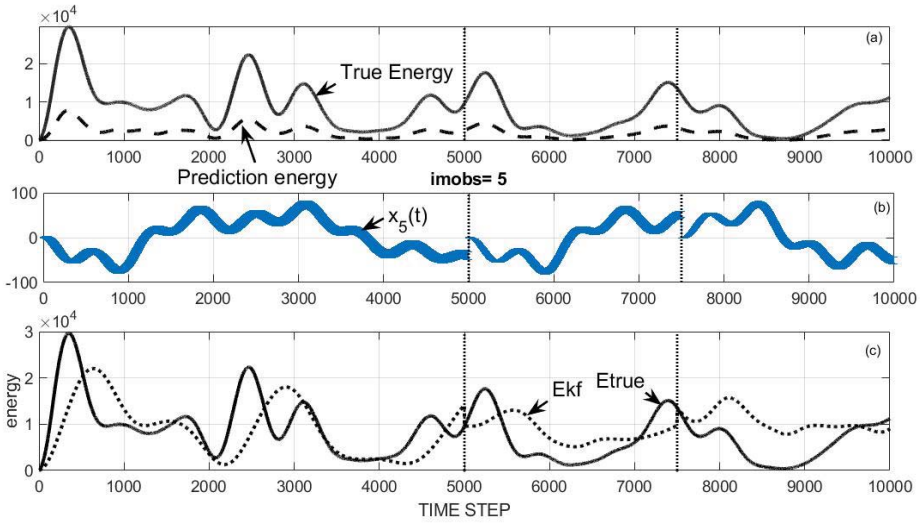

Figure 4: (a) Energy for the 3-mass-spring oscillator system ($\mathcal{E}(t)$) and for the prediction model showing the lower energy in the latter. Vertical lines are the time step when observations become available. (b) Estimated position for velocity in the first mass ($\dot{\xi}_1(t) = x_5(t)$) from the Kalman filter and showing the jump at the two times where there are complete *near-perfect* data. Standard error bar is shown from $\mathbf{P}(t)$. (c) $\mathcal{E}(t)$ and $\tilde{\mathcal{E}}(t)$ from the Kalman filter and showing the jumps at the observation times as well as the deviations following the observations. {osc_allobs_en

differing in the particular choice of noise value in each one and tabulating the resulting range. These uncertainties can be used to calculate the significance of any apparent trend in $\mathcal{E}(t)$ and although the result is not displayed here, use of reliable uncertainties can make an obvious important change in any inference about means and trends. In these examples, the observational errors are intentionally made relatively small, with no implications for what could be the case in geophysically realistic cases.

Notice that even in the observation interval, the estimated mechanical energy remains too low. This bias error is a systematic one owing to the availability of observations only of the velocity of one of the masses. Even if the observations are made perfect ones (not shown), this bias error in the energy persists.

As seen in the figure, with full-rank, near-perfect observations the elements of $x_i(t)$ and the total energy are forced to near the correct values at the two observation times, τ_i, but do diverge in following times.

A Fixed Position

Exploration of the dependencies of energies of the mass-spring system is interesting and a

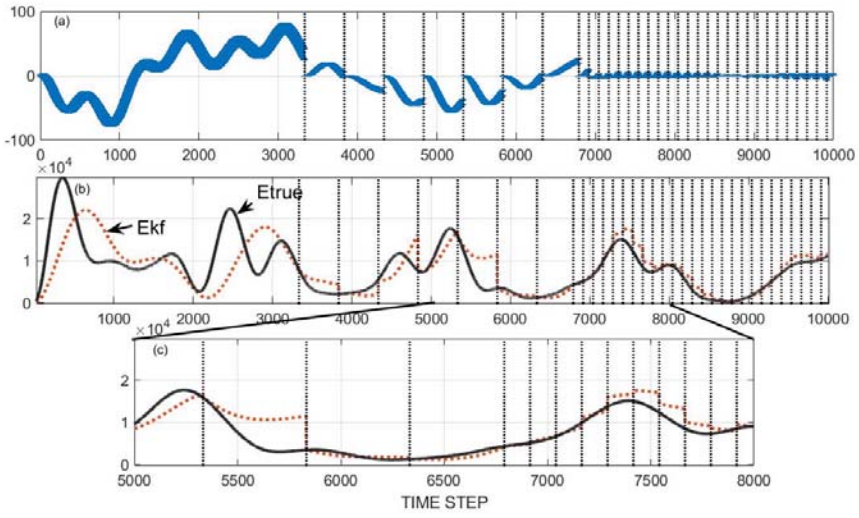

Figure 5: (a) $\tilde{x}_5(t) - x_5(t)$ and the same as Fig. 4b except with the observations shown at the times of the vertical dotted lines.(b) Estimated energy in the Kalman filter estimate when observations are available at times of the vertical dotted lines. (c) Expanded portion of (c). Note that the observational errors were here purposely made comparatively small relative to the signals. {osc_allobs_2d

great deal more can be said. Turn however, to a somewhat different invariant: suppose that one of the mass positions is fixed, but with value unknown to the analyst. A significant literature exists devoted to finding changes in scalar quantities such as global mean atmospheric temperatures, or oceanic currents, with the Atlantic Meridional Overturning Circulation (AMOC) being a favorite focus. These quantities are typically sub-elements of complicated models involving very large state vectors. With this very simple mass-spring oscillator system, it is useful to consider a situation in which an element is a constant, an invariant, but which must be determined from the sequential estimation procedure.

Using the same situation as above, added constraints, that $x_3(t) = \xi_3(t) = 2, x_6(t) = \dot{\xi}_3(t) = 0$, that is, an unmoving, fixed displacement in mass 3, are used in computing the true state vector. The observations are the velocity of moving mass $i = 2$, with similar noise in the interval shown in Fig. 6 . The question is whether one can infer accurately that $\xi_3(t)$ is a constant through time? Fixing $\xi_3(t) = 2$ does change all the true variables $\mathbf{x}(t)$ from the values they take without these extra constraints. Note that the fixed displacement means that the potential energy can never vanish. The resulting estimate for the position, $\tilde{\xi}_3(t)$, is shown in Fig. 6 and includes a significant error at all times.

Position variation occurs even during the data dense period and arises both from the entry of the data and the noise in the observations of $\dot{\xi}_2(t)$. An average taken over the two-halves

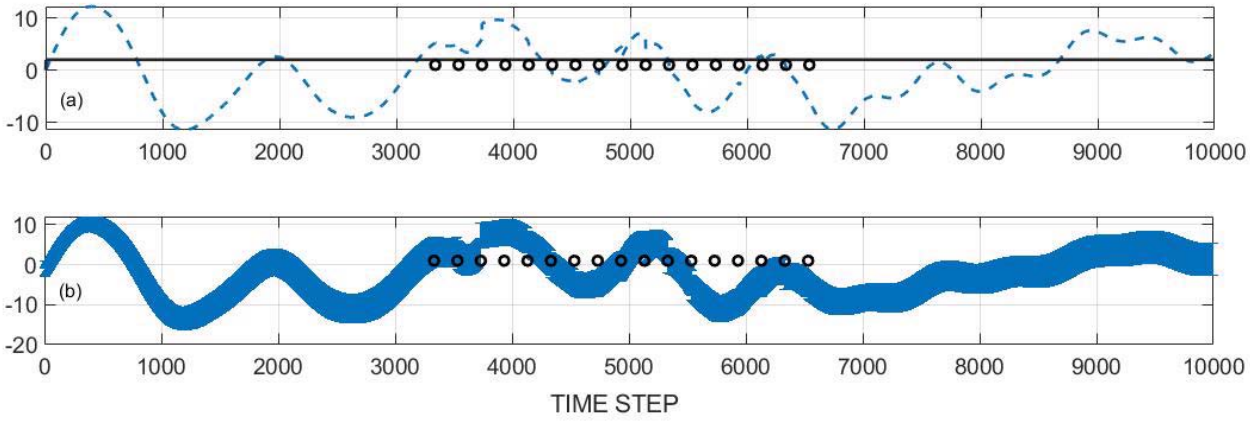

Figure 6: (a) Correct value of the constant displacement $\xi_3(t)$ (solid line), and the estimated value from the KF calculation (dashed line). Dots are the observation times. (b) Difference $\tilde{\xi}_3(t) - \xi_3(t)$ and one standard error bar computed from the matrix Riccati equation.

{xhatfx3_xfx3.

of the observation interval might easily lead to the erroneous conclusion that a decrease had taken place. Such an incorrect inference can be precluded by appropriate use of the computed uncertainties (Fig. 6). ≫

Observations of Averages

Consider now a set of observations of the average of the position of masses 2 and 3, and of the average velocity of masses 1 and 2, mimicking the type of observations that might be available in a realistic setting. Again for simplicity, the observations are very accurate and occur in the two-different sets of periodic time intervals The results are in Fig. 7. Position estimates shown are good, but not perfect, as is also true for the total energy. Visually it is clear that the energy estimate carries oscillatory power with the periodicity of the oncoming observations intervals and appears in the spectral estimate (not shown) with excess energy in the oscillatory band and somewhat low energy at the longest periods. Irregular spacing would introduced a potentially complex spectrum in the result.

A more general discussion of nullspaces involves that of the weighted $\mathbf{P}(\tau, -)\mathbf{E}^T$ appearing in the Kalman gain. If $\mathbf{E}$ is the identity, and $\mathbf{R}(\tau)$ has sufficiently small norm, all elements of $\mathbf{x}(\tau)$ are resolved. If the noise is uniform in all elements of $\mathbf{y}(\tau)$, the resolution analysis of the observations is also uniform and uninteresting. In the present case, with $\mathbf{E}$ having two

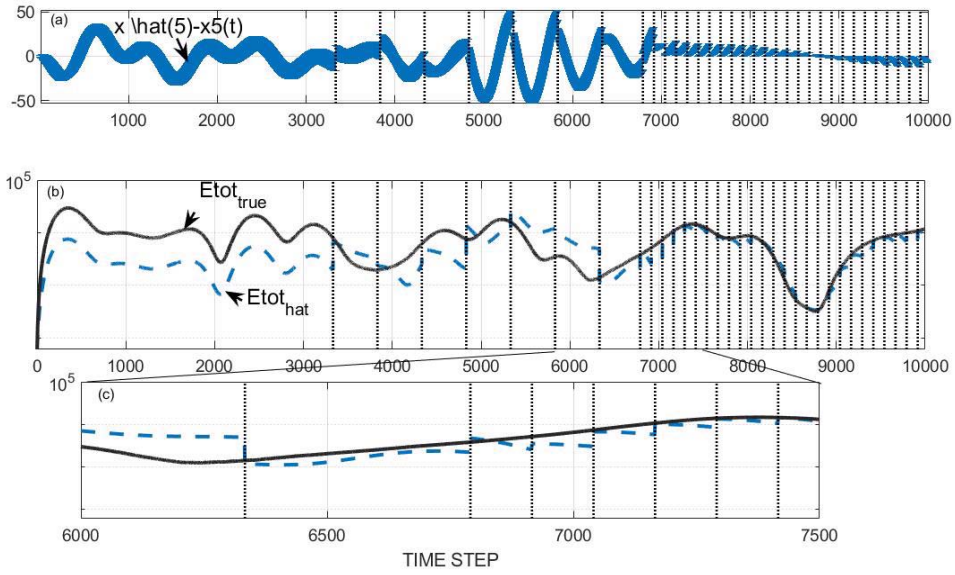

Figure 7: (a) Results for position estimate difference $\tilde{x}_5(t) - x_5(t)$ with standard error from the KF when observations were of the average of the two positions $x_2(t), x_3(t)$ and the two velocities, $x_4(t), x_5(t)$ at the times shown. (b) Total energy corresponding to the situation in (a). (c) Expanded portion of (b) showing the artificial periodicity in energy from the combination with observations. {osc_avgobs_z5

rows, corresponding to the observations of the averages of two-mass positions and of two velocity positions, the resolution analysis is more structured. With

$$\mathbf{E} = \left\{ \begin{array}{cccccc} 0 & 1/2 & 1/2 & 0 & 0 & 0 \\ 0 & 0 & 0 & 1/2 & 1/2 & 0 \end{array} \right\} \tag{26}$$

a singular value decomposition $\mathbf{E} = \mathbf{USV}^T = \mathbf{U}_2\mathbf{S}_2\mathbf{V}_2^T$, produces two non-zero singular values, and $\mathbf{U}_2$ etc. carries the first two columns of the matrix. At rank 2, the resolution matrices $\mathbf{T}_{U,}\mathbf{T}_V$ based on the $\mathbf{U}, \mathbf{V}$ vectors respectively and the standard solution covariances are easily computed (W06). $\mathbf{A}$ distributes information about the partially determined x_i throughout all masses via the dynamical connections as contained in $\mathbf{P}(\tau)$. Bias errors require specific, separate analysis.

Green Function Analysis of the Innovation Response

The innovation form of equations provides a convenient analysis method for determining the memory duration of varying observations. Define an innovation *matrix,*

$$\mathbf{y}(t) - \mathbf{E}(t)\,\mathbf{x}(t) = \mathbf{D}_\delta(t, j) = \delta_{t,\tau}\boldsymbol{\delta}_{ij} \tag{27}$$

that is, $\mathbf{D}_\delta$ is a matrix of Kronecker deltas of the difference $D_{ij}(\tau) = \delta_{t,\tau}\boldsymbol{\delta}_{ij} = y_j(\tau) - \sum_r E_{ir}(\tau)\, x_r(\tau)$. The solutions to the equation are the columns of the Green function matrix,

$$\mathbf{G}(t) = \mathbf{A}\mathbf{G}(t-\Delta t) + \mathbf{K}\mathbf{D}_\delta(t),\ t = m\Delta t. \tag{28}$$ {green1}

$\mathbf{K}$, now fixed in time, is sought as an indication of a delta impulse effects of observations on the prediction model at time τ.

Define the scalar complex variable,

$$z = \exp(-i2\pi s\Delta t), -1/2\Delta t \leq s \leq 1/2\Delta t. \tag{29}$$

Then the discrete Fourier transform of Eq. (28) (the $z-$transform—a matrix polynomial in z) is,

$$\hat{\mathbf{G}}(z) = (\mathbf{I}-z\mathbf{A})^{-1}\mathbf{K}\hat{\mathbf{D}}_\delta(z). \tag{30}$$ {ghat1}

The norm of the variable $(\mathbf{I}-z\mathbf{A})^{-1}$ defines the "resolvent" of $\mathbf{A}$ in the full complex plane (see Trefethen and Embree, 2005), but here, only $|z| = 1$, is of direct interest, that is only on the unit circle. The full complex plane carries information about the behavior of $\mathbf{A}$, including stability.

Here $\hat{\mathbf{D}}(z) = \mathbf{I}z^\tau$ and,

$$\hat{\mathbf{G}}(z) = (\mathbf{I}-z\mathbf{A})^{-1}\mathbf{K}z^\tau \tag{31}$$

If a suitably defined norm of $\mathbf{A}$ is less than 1,

$$\hat{\mathbf{G}}(z) = (\mathbf{I}-z\mathbf{A})^{-1}\mathbf{K}z^\tau \approx \left(z^\tau\mathbf{I}+z^{\tau+1}\mathbf{A}+z^{\tau+2}\mathbf{A}^2 + z^{\tau+3}\mathbf{A} + ...\right)\mathbf{K} \tag{32}$$

and the solution matrix in time is the causal vector sequence (no disturbance before $t = \tau$) of columns of

$$\begin{aligned} \mathbf{G}(t) &= 0, t < \tau \\ &= \mathbf{A}^m\mathbf{K}(\tau),\ t = \tau + m\Delta t \\ m &= 0, 1, 2, ... \end{aligned} \tag{33}$$

$\mathbf{G}$ can be obtained without the $z-$transform, but the frequency content of these results is of interest.

4.1 Varying Data Density

As was conspicuous above, data density in time influences the accuracy of estimates of $\mathcal{E}(t)$. Consider the behavior of the energy estimate as the density of observations varies in time. Fig. 8 displays the RMS difference between the estimated energy over the observation intervals (including non-observation times) as a function of the number of data points included. Compare Fig.

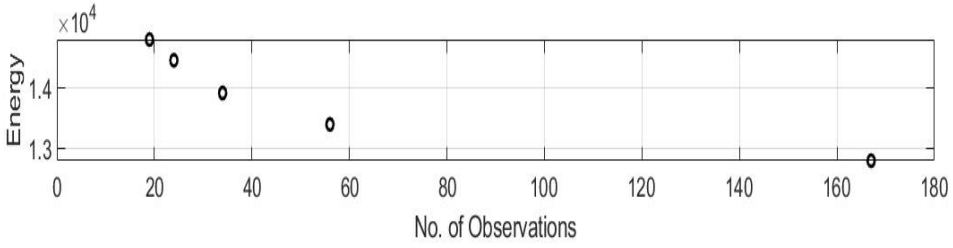

Figure 8: RMS difference $\mathcal{E} - \mathcal{E}true$ as a function of the number of data points in the time interval used. {osc_e_varying

5. Similar results will apply e.g., to changing the observational accuracies (and biases) as well as the number of observations of individual or average elements $x_i(t)$. With these parameters, the change is not large relative to the background, but as a climate analogue, the importance would depend upon the physical significance of a small change (e.g., Wunsch, 2020).

4.2 The Uncertainties

The structure of the uncertainties depends upon both the model and the detailed nature of the observations. Consider $\mathbf{P}(t)$ for $t = 3523 = m\Delta t$, and one time-step into the future, Fig. 9b,c, just before and after some observations becomes available..

Notice that changing variances along the diagonal, and the sometimes strong covariances implied amongst the different elements of $\hat{\mathbf{x}}(t)$ after 10 observations have been used. One of the eigenvalues of $\mathbf{P}(t)$ is almost zero, meaning that $\mathbf{P}(t)$ is singular. In this case, the only observation was relatively accurate—one of the velocity of the second mass. The eigenvector corresponding to the zero eigenvalue is close to 1 in position 5 (corresponding to the observed $\dot{\xi}_2 = d\xi_2/dt$) and zero elsewhere. The implication is, that because very good observations were made of $\dot{\xi}_2$, its uncertainty almost vanishes here, and a weighting of values by $\mathbf{P}(t)^{-1}$ would give it a near infinite weight at that time.

5 A Fixed-Interval Smoother

As already noted, most physical models in use include some form of invariant principles, including quadratic ones related to energy, linear ones related e.g. to vorticity or to positions or flows. These principles are violated whenever the model is combined with data. A reasonable inference for science generally is that no system that violates conservation rules for mass or energy etc., can be physically understood in a meaningful way. The need for system descriptions over finite intervals that do satisfy such principles leads to the notion of "smoothers"—in which the state

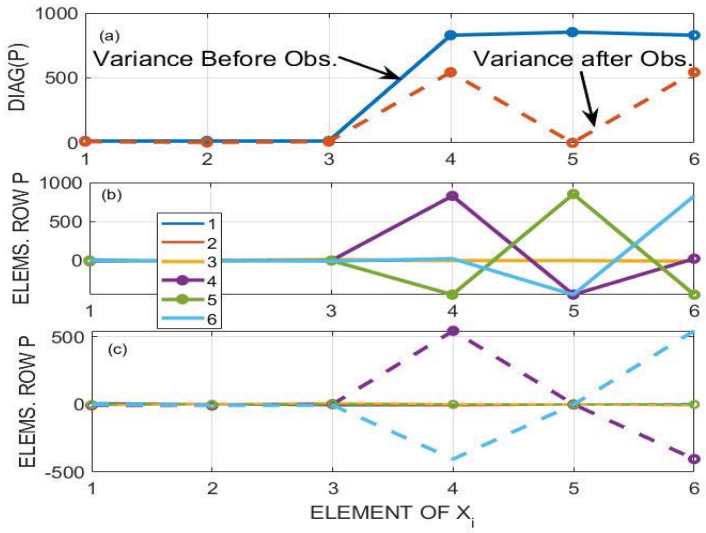

Figure 9: Only observation is *velocity* of mass 2. (a) Diagonal element of $\mathbf{P}(t)$ just prior to an observation and after 10 observations of $x_5(t)$ have been obtained. (b,c) Rows of $\mathbf{P}(t)$, corresponding to the two times in (a).

{osc_p_hat.jpg

vector over a finite interval simultaneously satisfies a modified model and the data within error bars such that no invariant violation occurs.

The idea of smoothers is again a control theory construct (see Liebelt, 1967, Anderson and Moore., 1979, Brogan, 1991, W06 among many others), and algorithmically a number of different approaches for linear systems have been developed. A particularly useful one is called the RTS (for authors Rauch, Tung, Striebel) and which is built under the hypothesis that a KF calculation has already been used over a time interval $0 \le t \le t_f$ with the results, including all of the state vectors and $\mathbf{P}$ matrices, stored.

The basic notion is to find the corrections, $\mathbf{\Gamma}\tilde{\mathbf{u}}(t)$, the controls, such that the suitably modified prediction model produces a new, the third, state estimate $\tilde{\mathbf{x}}(t,+)$ obeying the model time-evolution while simultaneously, consistent within error bars, of all the data. In that way, the usual invariants of energy etc., are restored. $\tilde{\mathbf{x}}(t,+)$ is generally a better estimate than is $\tilde{\mathbf{x}}(t)$ because it "knows" of the occurrence and values of observations *future* to the time t and accounts for them. The algorithm (see Appendix B, P2) has a somewhat complicated appearance because the sequential estimates of $\tilde{\mathbf{x}}(t)$ are correlated with each other, and recombining them in any way involves accounting for that correlation. Application is made in Part 2 to a slightly more geophysically identifiable example.

6 Some Comments on Part 1

Errors, random and systematic, can evidently occur in a sequential filtering or prediction system owing to a large number of elements, even in this simple mass-spring oscillator system. Apart from those associated with writing a linear model, any distortion in initial conditions, $\tilde{\mathbf{x}}(0)$, initial condition uncertainties $\mathbf{P}(0)$, in the data, and in the data error covariances, $\mathbf{R}(\tau)$, will lead to distortions in estimates of invariants ranging from those of position or velocity to linear and quadratic physical quantities such as energy and momenta. A subset of the possibilities has been explored here. The main point is that for purposes of determining trends in quantities such as positions, velocities, energies, or concentrations, the temporal and physical distributions of the data can imply false trends and even periodicities. All of these can be accounted for by finding and using appropriate uncertainties.

It will be clear that calculation of Kalman filter estimates, even for linear systems, involves the computation through time of the uncertainty matrices $\mathbf{P}(\tau,-), \mathbf{P}(\tau)$ in such a way that the gain operator $\mathbf{K}(\tau)$ evolves through time. If the state vector has dimension N, computation of $\tilde{\mathbf{x}}(t)$ involves running the model once at each time step. On the other hand, calculation of $\mathbf{P}$ involves (Eq. A1) running the model N^2 times for each time-step (once for each column and row on the $\mathbf{P}$ matrix). This calculation is prohibitive for all realistic (quasi-global) climate or related models (with N approaching 10^{10}) and consequently most such calculations replace the time-dependent behavior of $\mathbf{K}(t)$ with an ad hoc, time-fixed matrix, $\mathbf{K}_0$, in what amounts to a predictor-corrector system. Rigorous KF systems are thus almost never used. From the above experiments, it should be clear that the implied errors through time when data are used can arise from a large number of distortions potentially buried in the choice of $\mathbf{K}_0$. Trends of any sort, or their absence, will be a consequence of $\mathbf{K}_0$ (see Appendix A, P1).

Appendix A, Part 1. Kalman Filter, and Predictor-Corrector Approximations

Commonly, climate and other models are almost always written so that the physical conservation rules for energy etc., are satisfied to a good approximation. Without such conservation constraints, be they physical, chemical, or biological, interpretation of an "open" system can become impossible.[3] Let $\mathbf{P}(\tau,-)$ represent the error covariance (uncertainty) of $\tilde{\mathbf{x}}(\tau,-)$:

$$\begin{aligned}\mathbf{P}(t,-) &= \left\langle (\tilde{\mathbf{x}}(t,-)-\mathbf{x}(t))(\tilde{\mathbf{x}}(t,-)-\mathbf{x}(t))^T \right\rangle \\ &= \mathbf{A}(t)\mathbf{P}(t-\Delta t)\mathbf{A}(t)^T + \mathbf{\Gamma}(t-\Delta t)\mathbf{Q}(t-\Delta t)\mathbf{\Gamma}(t-\Delta t)^T,\end{aligned} \tag{A1}$$ {pminus}

a matrix Riccati equation, which is just the sum of the error covariance propagated from the predicted estimate, plus that generated by unknown forcing, etc., elements, $\mathbf{u}(t)$, with $\mathbf{Q}(t) = \left\langle \mathbf{u}(t)\mathbf{u}(t)^T \right\rangle$, the bracket defining an ensemble average. (See any of numerous textbooks cited above.) The notation $\mathbf{Q}(t)$ is used as a reminder that $\mathbf{u}(t)$ represents the unknown errors in $\mathbf{q}(t)$. Inaccuracies in this equation are discussed by Konstantinov et al. (1993), Zhou et al. (2009) and $\mathbf{P}$ must always itself be regarded as an estimate, not "truth." Note that precision, rather than accuracy, is being omitted here.

A useful conceptual generalization of these methods is to create ensembles of solutions e.g., generated by random selection of different initial conditions from the probability density of the initial conditions (e.g., Evensen, 2009) and then using the results to calculate variances of the corresponding solutions. Difficulties lie with the very large number of elements subject to random and systematic errors, choice of the correct probability densities, and the usual very small number of ensemble members feasible to compute relative to the dimension e.g., of $\mathbf{x}(t)$. For trend determination accurate knowledge of the overall uncertainties remains important.

Steady-State and Asymptotics

Time sequence equations starting at $t = 0$ (however defined) undergo a general transient behavior. For simplifying purposes, and following much of the literature, assume that a steady-state has been reached, so that the linear prediction model and the innovation equation have become,

$$\tilde{\mathbf{x}}(t,-) = \mathbf{A}\tilde{\mathbf{x}}(t-\Delta t,-) + \mathbf{Bq}(t-\Delta t) \tag{A2}$$ {A2}

$$\tilde{\mathbf{x}}(t) = \mathbf{A}\tilde{\mathbf{x}}(t-\Delta t,-) + \mathbf{Bq}(t-\Delta t) + \mathbf{K}[\mathbf{y}(t) - \mathbf{Ex}(t)], \tag{A3}$$ {A3}

[3] The existence and use of the information contained in such *a priori* models, kinematic, thermodynamic, biological, chemical, and otherwise distinguishes this approach from some attempts to use machine learning to deduce a fully *a posteriori* model. The result of Pitandosi (2018) is thus a challenging one.

respectively, with no time-dependence in $\mathbf{A}, \mathbf{B}$, or $\mathbf{K}$. Time-dependence remains in $\tilde{\mathbf{x}}(t)$ but it can be statistically stationary (labelled "wide" or "weak" depending on the literature). The steady-state error covariance is

$$\mathbf{P}_\infty(-) = \mathbf{A}\mathbf{P}_\infty(-)\mathbf{A}^T + \mathbf{B}\mathbf{Q}\mathbf{B}^T, \tag{A4}$$ {pinf1}

$$\mathbf{P}_\infty = \mathbf{P}_\infty(-) - \mathbf{P}_\infty(-)\mathbf{E}^T\left[\mathbf{E}\mathbf{P}_\infty(-)\mathbf{E}^T + \mathbf{R}\right]^{-1}\mathbf{E}\mathbf{P}_\infty(\tau,-), \tag{A5}$$ {pinf2}

an algebraic Riccati equation, and

$$\mathbf{K}_\infty = \mathbf{P}_\infty(-)\mathbf{E}^T\left[\mathbf{E}\mathbf{P}_\infty(-)\mathbf{E}^T + \mathbf{R}\right]^{-1} \tag{A6}$$ {pinf3}

is also constant. Pitfalls lie in the accuracies of $\mathbf{P}_\infty$ and in $\mathbf{R}$.

Within a steady-state, the various moments can be computed. So for example, from the innovation state equation, the mean

$$\mathbf{m}_x = \langle\tilde{\mathbf{x}}(t)\rangle = \mathbf{A}\langle\tilde{\mathbf{x}}(t-\Delta t,-)\rangle + \mathbf{B}\langle\mathbf{q}(t-\Delta t)\rangle + \mathbf{K}_\infty\left[\langle\mathbf{y}(t) - \mathbf{E}\mathbf{x}(t)\rangle\right], \tag{A7}$$

or

$$\mathbf{m}_x = (\mathbf{I}-\mathbf{A})^{-1}\left[\mathbf{K}_\infty\ \langle\mathbf{y}(t) - \mathbf{E}\mathbf{x}(t)\rangle + \mathbf{B}\langle\mathbf{q}(t-\Delta t)\rangle\right] \tag{A8}$$

and thus depends directly upon any bias errors in $\mathbf{y}(t)$ and $\mathbf{E}$, and the accuracy of $\mathbf{K}_\infty$. It will be sensitive directly to the structure and rank of $\mathbf{I}-\mathbf{A}$.

Predictor-Corrector Methods

Rigorous Kalman filters are widely used in many applications. In climate systems they are almost never used, despite claims to the contrary, because of the computational cost of Eq. (A1). Instead, $\mathbf{K}(\tau)$ is replaced by an ad hoc, often constant, matrix, $\mathbf{K}_{pc}$, and in which Eq. (6) is a predictor-corrector system,

$$\tilde{\mathbf{x}}(\tau) = \tilde{\mathbf{x}}(\tau,-) + \mathbf{K}_{pc}\left[\mathbf{y}(\tau) - \mathbf{E}(\tau)\mathbf{x}(\tau)\right]. \tag{A9}$$ {predcorrector

$\mathbf{K}_{pc}$ would be substituted for $\mathbf{K}_\infty$ in the previous equations whether derived from the formal solution Eq. (7) or not. As with the true KF, $\tilde{\mathbf{x}}(\tau)$, once combined with data, using $\mathbf{K}_{pc}$, no longer satisfies the prediction model equations, having undergone a jump in values at time τ. As with the true KF, the predictor-corrector system can be written in innovation form, showing the apparent forcing by data.

Fig. 10 depicts the variation in some elements of the Kalman gain matrix for a set of observations at the places shown. Some elements do tend to become nearly constant at the data

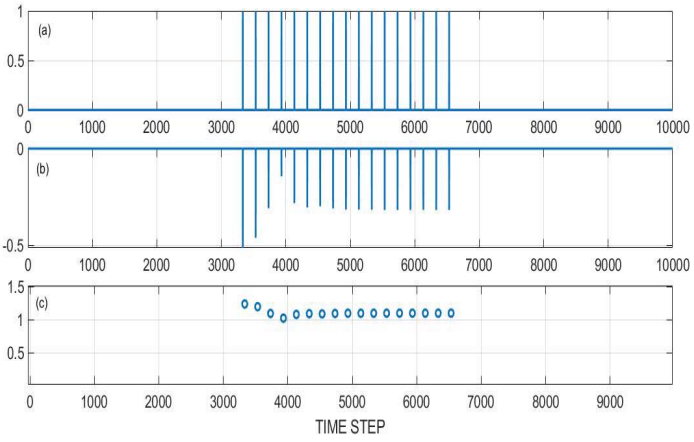

Figure 10: Kalman gain matrix elements through time and its norm. (a) $\mathbf{K}_{55}(t)$, which is the gain in $x_5(t)$ for an observation of $x_5(t) = \dot{\xi}_2(t)$.(b) $\mathbf{K}_{65}(t)$—the gain in $x_6(t) = \dot{\xi}_3(t)$ for an observation of $x_5(t)$. (c) $\|\mathbf{K}(t)\|$, the 2−norm. Only $x_5(t) = \dot{\xi}_2$ was observed. Zero values interlace the observation times.

{osc_kgain5.jp

times, while others continue to show a structure. Whether choosing $\mathbf{K}_{pc}$ from one particular time is adequate will be very much problem dependent.

Part 2. Barotropic Rossby Waves

7 Introduction

Part 1 (P1) of this paper discussed the impact of time-varying observational data on simplified examples of sequential estimation systems in time. The focus was on the behavior of quantities that can be regarded as intrinsically conserved or constant in well-understood problems. As in P1, the expressions "conserved quantities" or "(potential) invariants" are used for those elements which would be internally unchanging were there no dissipation nor external sources/-sinks/forcings. These conservative quantities include energy, total inventories, vorticity, etc. Examples were based on mechanical energy and positions in mass-spring oscillators. Identifying and calculating these conservative properties is fundamental to understanding of any physical system. Estimation concepts can be extended to various properties believed constant over some finite time interval—the time-independent transport of a current system being one example.

In linear systems satisfying a comprehensive set of physical and statistical assumptions, the

Kalman filter (KF) provides a basis on which to make an optimal prediction at future time steps—a prediction employing all of the known kinematic/dynamical model elements as well as all of the data available to that time. Analogous algorithms, some best-regarded as predictor-corrector methods, can greatly reduce the computational load, but at the possible expense of significantly distorted estimated and predicted values. Climate reanalyses are commonly based on these simplified methods.

Consider now the problem of reconstruction of invariants over the entire time-span of estimation, building on the sequential analysis and notation of P1. Realism is still not the goal—rather it is the demonstration of various elements making up estimates in simplified settings in what can be regarded as an exercise in geophysical fluid statistics (GFS). In particular, evaluation of the importance of deviations, large or small, of the estimates from true values can only be made in the context of a particular physical situation (in some cases a 1% error is the maximum tolerable; in others 50% or even an order of magnitude would be regarded as still useful).

8 The Smoothing Problem

A variety of smoothing approaches exists (e.g. Anderson and Moore, 1979; Goodwin and Sin, 1984; Stengel, 1986). Here the "fixed interval" smoother is of most interest. The fundamental idea is straightforward: to find a weighted least-squares fit of the invariant-conserving model (Eq. 2) to the data Eq. (4) at the sampling times.

8.1 RTS Smoother

Consider the sequential method usually known as the Rauch-Tung-Striebel (RTS) smoother described in Appendix C (other algorithms exist), in which the assumption is made that the KF has already been used, rigorously, over the finite interval $0 \leq t \leq T_{dur}$, producing the estimates denoted $\tilde{\mathbf{x}}(t,-), \tilde{\mathbf{x}}(t)$ with their corresponding uncertainty covariances $\mathbf{P}(t,-), \mathbf{P}(t)$. At this stage, no further discussion of the data occurs: all information contained in the observations has been exploited by the KF and is encompassed in $\tilde{\mathbf{x}}(t)$ and its uncertainty $\mathbf{P}(t)$. What has *not* been exploited in an estimate $\tilde{\mathbf{x}}(t), \mathbf{P}(t)$, is the information contained in data that were obtained *afterwards*, $t + m\Delta t > t$, *but that information is present in any later estimates* $\tilde{\mathbf{x}}(t + m\Delta t), \mathbf{P}(t + m\Delta t)$.

The resulting RTS algorithm is more complex appearing than is the KF, because all of the later estimates have a finite correlation with the previous ones, and they cannot be simply combined without first removing that correlation. (The pure scalar state vector is readily analyzed without any matrix/vector algebra and is written out in P1, Appendix C.) In the same notation,

and repeating the equations of Appendix B,

$$\tilde{\mathbf{x}}(t,+) = \tilde{\mathbf{x}}(t) + \mathbf{L}(t+\Delta t)\ [\tilde{\mathbf{x}}(t+\Delta t,+) - \tilde{\mathbf{x}}(t+\Delta t,-)]\,,$$
$$\mathbf{L}(t+\Delta t) = \mathbf{P}(t)\mathbf{A}(t)^T\,\mathbf{P}(t+\Delta t,-)^{-1},$$

$$\mathbf{P}(t,+) = \mathbf{P}(t) + \mathbf{L}(t+\Delta t)\,[\mathbf{P}(t+\Delta t,+) - \mathbf{P}(t+\Delta t,-)]\,\mathbf{L}(t+\Delta t)^T,$$
$$\mathbf{Q}(t,+) = \mathbf{Q}(t) + \mathbf{M}(t+\Delta t)\,[\mathbf{P}(t+\Delta t,+) - \mathbf{P}(t+\Delta t,-)]\,\mathbf{M}(t+\Delta t)^T,$$

involving the estimated $\tilde{\mathbf{x}}(t+\Delta t)$, $\mathbf{P}(t+\Delta t,-)$, $\mathbf{P}(t+\Delta t)$ at a formally future time, $t+\Delta t$. The $+$ in the argument is used to label the estimates of these variables as now having employed the formally *future* data. One can examine putative steady-state behavior of the smoothing equations, to the extent it is plausible.

For all these methods, a potentially very important, but implicit, assumption is $\left\langle \mathbf{n}\,(t)\,\mathbf{n}\,(t')^T \right\rangle = \mathbf{0}$, $t \neq t'$, that is observational noise is uncorrelated over time. Similarly, $\left\langle \mathbf{u}\,(t)\,\mathbf{u}\,(t')^T \right\rangle = \mathbf{0}$, $t \neq t'$. If the assumptions fail, a general approach is to model the structures of $\mathbf{n}\,(t)$, $\mathbf{u}\,(t)$ as part of the problem—essentially augmenting the state vectors.

8.2 Green Function of Smoother Innovation

As with the innovation equation for filtering, Eq. (B1a) introduces a disturbance into the previous estimate, $\tilde{\mathbf{x}}\,(t)$, in which the structure of $\mathbf{L}\,(t)$ will determine the magnitude and time scales of observational "disturbances" propagated *backwards* in time. It is an indication of how much influence later measurements will have on earlier estimates. Suppose that the KF has been run to time $t = t_f$ so that $\tilde{\mathbf{x}}\,(t_f,+) = \tilde{\mathbf{x}}\,(t_f)$, which has the only measurement. Let the innovation, $\tilde{\mathbf{x}}(t_f,+) - \tilde{\mathbf{x}}(t_f,-)$, be a matrix of δ functions in separate columns,

$$\mathbf{D} = \delta\,(t - t_f)\,\mathbf{I}_N \tag{34}$$

then a backwards-in-time matrix Green function is,

$$\mathbf{G}\,(t) = \mathbf{L}(t)...\mathbf{L}\,(t_f - \Delta t)\,\mathbf{L}\,(t_f) \tag{35}$$

The various time-scales embedded in $\mathbf{L}$ depend upon those in $\mathbf{A}, \mathbf{P}\,(t,-)\,, \mathbf{P}\,(t)$ and with many observations including those of the observation intervals, and any structure in the observational noise. Similarly, the control modification will be determined by $\mathbf{P}(t+\Delta t,-)^{-1}$ if $\mathbf{Q}(t)\mathbf{\Gamma}(t)^T$ are constant in time.

9 Example: Rossby Wave Normal Modes

P1 showed the generic character of linear estimation problems, with dependencies on uncertainties, data densities, and accuracies etc. A more recognizably geophysical example now used is the flat-bottom, linearized β-plane Rossby wave system, whose governing equation is,

$$\frac{\partial \nabla^2 \psi_1}{\partial t} + \beta \frac{\partial \psi_1}{\partial x} = q\left(t, x, y\right), \tag{36}$$ {rossby1}

in a square beta-plane basin of horizontal dimension L. This problem is taken to be representative of those involving both space and time structures, including boundary conditions. (Spatial variables x, y should not be confused with the state vector or data variables). Eq. (36) and other geophysically important ones are not self-adjoint, and the general discussion of quadratic invariants leads inevitably to adjoint operators (see Morse and Feshbach, 1953 or for bounding problems—Sewell, 1987, Chs. 3,4).

The closed-basin problem was considered by Longuet-Higgins (1964 and later). Pedlosky (1965) and Lacasce (2002) provide helpful discussions of normal modes) and relevant observational data are discussed by Luther (1982), Woodworth et al. (1995), Ponte (1997), and others. The domain is $0 \leq x \leq L_x$, $0 \leq y \leq L_y$ with boundary condition $\psi = 0$ on all four boundaries.

Introduce non-dimensional primed variables, $t' = ft, x = Lx'$, $q = q_0 q'$, $\psi_1' = (a^2/f)\psi_1$. f, β are evaluated at 30°N. Letting a be the Earth radius, and $\beta = \beta' a/f = 1.7$, the non-dimensional equation becomes,

$$\frac{\partial \nabla'^2 \psi_1'}{\partial t'} + \beta' \frac{L}{a} \frac{\partial \psi_1'}{\partial x'} = \frac{L^2}{f} q\left(t', x', y'\right) = q', \tag{37}$$

choosing further $L = a$, and then omitting the primes from here on except for β',

$$\frac{\partial \nabla^2 \psi_1}{\partial t} + \beta' \frac{\partial \psi_1}{\partial x} = q\left(t, x, y\right). \tag{38}$$

Hairer et al. (2006) describe numerical methods that specifically conserve invariants, but these are not discussed here. This system was used by Gaspar and Wunsch (1989) for a demonstration of sequential estimation using altimetric data. Here a different state vector will be used.

The solution used is the sum over normal modes satisfying the boundary conditions, $\psi_1 = 0$,

$$\psi_1\left(x, y, t\right) = \sum_n \sum_m \exp\left(-i\sigma_{nm} t\right) c_{nm} e^{-i\beta' x/\sigma_{nm}} \sin\left(n\pi x\right) \sin\left(m\pi y\right),$$

and obeying the non-dimensional dispersion relation,

$$\sigma_{nm} = -\frac{-\beta'/2}{\sqrt{\left(n\pi\right)^2 + \left(m\pi\right)^2}}$$

where c_{nm} is a coefficient dependent upon initial conditions and any forcing present; see especially, Pedlosky (1965).

The problem is now made a bit more interesting by addition to ψ_1 of a *steady* component, the solution, $\psi_s(x,y)$ from Stommel (1948) whose governing equation in this non-dimensional form is, where R_a is a Rayleigh friction,

$$R_a' \nabla^2 \psi_s + \beta' \frac{\partial \psi_s}{\partial x} = \sin \pi y, \tag{39}$$

$R_a' = R_a/f$, here written in the simple boundary-layer/interior approximation,

$$\psi_s = e^{-x\beta'/R_a'} \sin \pi y + (x-1) \sin \pi y, \tag{40}$$

which leads to a small error in the eastern boundary condition. The $\sin \pi y$ arises from Stommel's assumed time-independent wind-curl.

For the time-dependent components, the state vector is,

$$\mathbf{x}(t) = \mathrm{vec}\{c_p(t)\},$$

where p is a linear ordering of n, m of total dimension $N \times M = N_{state} - 1$, which is equal to the number of n times the number of m, and the state transition equation is,

$$x_j(t+\Delta t) = \exp(-i\sigma_j \Delta t)\, x_j(t) + q_j(t), \quad j = 1, .., N_{state} - 1,$$

with a complex, diagonal state transition matrix, $\mathbf{A}_2$= diag $(\exp(-i\sigma_p \Delta t))$, square of dimension $N_{state} - 1$. A small, numerical dissipation is introduced, multiplying $\mathbf{A}$ by $exp(\text{-}bt), b > 0$, to accomodate loss of memory, e.g., as a conventional Rayleigh dissipation. Some special care in computing covariances must be taken when using complex state vectors and transition matrices (Schreier and Scharf, 2010).

The time-independent flow is included as,

$$x_{Nstate}(t+\Delta t) = x_{Nstate}(t), \tag{41}$$

and again,

$$\mathbf{x}(t+\Delta t) = \mathbf{A}\mathbf{x}(t) + \mathbf{B}\mathbf{q}(t), \tag{42}$$ {canon1}

where complex $\mathbf{A}$ is the same as $\mathbf{A}_2$ except with an added zero row and column , and a single non-zero element, $\mathbf{A}(N_{state}, N_{state}) = 1$. Eq. (42) here is taken to exactly describe the putative "truth". $q_{N_{state}}(t) = 0$, because the Stommel solution has a steady wind.

Consistent with the analysis in Pedlosky (1965), no westward intensification exists in the normal modes, which decay as a whole. Rayleigh friction of the time-dependent modes is permitted to be different from that in the time-independent mean flow—a physically acceptable

situation. The value $b = \sigma_{11}/30 = 1.8 \times 10^{-3}$ is used. No particular realism is intended here in the choices of numerical amplitudes, data properties etc. They are chosen only to demonstrate the estimation issues.

If $\mathbf{q}(t) = 0$ and with no dissipation, then following P1, Eq. (36) has several useful invariants: the quadratic invariant of the kinetic energy and of the "energy" in ψ—$\mathbf{x}^T(t)\,\mathbf{x}(t)$ (complex transpose); and the linear invariant of the vorticity or circulation—when integrated over the entire basin domain. Estimates of the quadratic and linear invariants will depend explicitly on initial conditions, forces, distribution and accuracy of the data, and the covariances and bias errors assigned to all of them.

Eq. (42) is here taken to be "truth" and to generate the correct fields. As would be necessary in practice, a "prediction" model is introduced as

$$\mathbf{x}_p(t + \Delta t) = \mathbf{A}\mathbf{x}_p(t) + \mathbf{B}\mathbf{q}_p(t). \tag{43}$$ {pred2}

with the only difference from the truth model in the initial conditions and forcings.

10 System with Observations

The problem is now posed of determining the transport of the western boundary current (WBC), which is here a constant (invariant) in the presence of *both* physical noise—the normal modes—and the random noise of the observations $\mathbf{y}(\tau_i)$. For determining the transport of the WBC, the presence of both natural noise (the time-dependent modes) and observational noise is analogous to the true physical circulation problem. Non-dimensional normal mode frequencies and periods for $n = 3, 4, 5$, $m = 4, 5, ..., 9$ are shown in Fig. 11. $\Delta t = 29, 1/b = 553$, $R'_a/\beta' = 0.29$

Initial modal amplitudes are taken to have a slightly "red" property. The field $\psi(t = 167\Delta t)$ is shown in Fig. 12, keeping in mind that apart from the time-mean ψ, the structure is the result of a particular set of random forcings.

Noisy observations, $\mathbf{y}(t)$, are taken at the positions in Fig. 12. The prediction model has the correct $\mathbf{A}$, but the magnitudes of the initial conditions are 20% too large, and the forcing field magnitude of q_p is 50% too small (the forcing is complex white noise).

Aliasing

In isolation, the observations will time-alias the field, if not taken at minimum intervals of 1/2 the shortest period present (here $4\Delta t$). A spatial-alias occurs if the separation is less that 1/2 the shortest wavelength present (here $\Delta y = 1/9$). Both these phenomena are present in what follows, but their impact is minimized by the presence of the time-evolution model. Times of assumed observation vary and are displayed below in the time-series results figures.

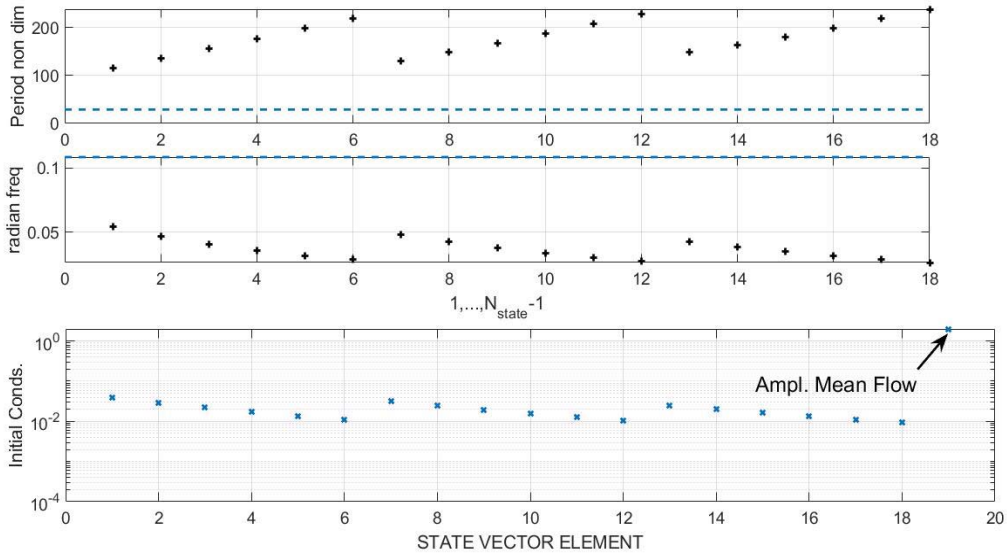

Figure 11: (a) Non-dimensional periods, grouped by increasing n, and then increasing m for fixed n with $n = 3, 4, 5$, $m = 4, 5, ..., 9$. Dashed line is the computational step, Δt. (b) Radian frequencies corresponding to the upper panel. (c) Logarithm of the initial conditions for the normal modes. {rossby_modes_

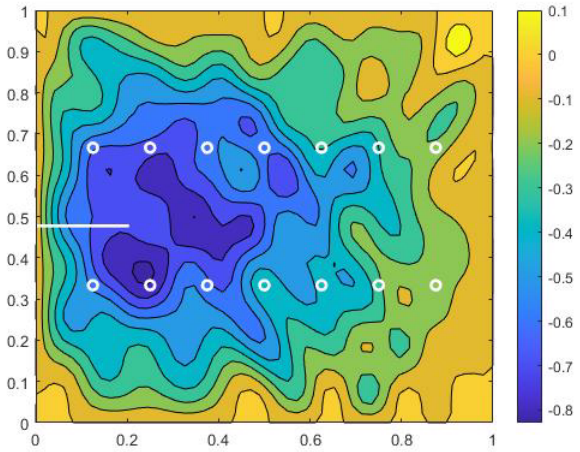

Figure 12: Stream function after 11 time steps of including both normal modes and the time–independent Stommel solution. At later times, the mean flow becomes difficult to visually detect in the presence of the growing normal modes under the forcing. White line segment is the distance over which the boundary current transport is defined, slightly shorter than the e^{-1} decay thickness of the boundary current. White circles indicate the assumed 14 available observational positions, fixed in time. {rossby_withme

11 Results: KF+RTS

11.1 KF Estimates

The RTS algorithm assumes that a proper KF result has been computed and the results stored. $\mathbf{P}(0) = \text{diag}_{Nstate}(1)$, initial condition uncertainty, and is uniform amongst the elements. Here, as shown in Fig. 13, *a priori* knowledge that higher frequencies have smaller initial values is not being used. $\mathbf{Q}(t) = \text{diag}(0.015)$ except for $x_{Nstate}(t)$ for which $Q_{N_{state},N_{state}}(t) = 0$, $\mathbf{R}(t) = \text{diag}_{Nobs}(0.6 \times 10^{-3})$. The system is run with the knowledge that the time-mean wind is truly constant. Observations are available spatially as in Fig. 12 at intervals, initially at $50\Delta t$ beginning at $t = 166\Delta t$ (Fig. 13) and then more densely at $25\Delta t$ spacing, a crude mimicking of observations becoming more dense with time. Observations cease prior to T_{dur}, mimicking a pure prediction interval following the observed states.

The energy, $\Phi(t) = \sum_{nm} |\alpha_{nm}(t)|^2$, in the time-dependent components is shown for the true value and the KF estimate in Fig. 13. It is a surrogate for the total system energy and is a quadratic variable. A slow increase is visible in the true value and in the prediction value with a levelling off at around time-step 200, again a combination of the dissipation and the white noise random walk increase. Until the first observation time, the predicted energy is identical to that of the KF, $\Phi_{pred}(t) = \Phi_{kf}(t)$, when the latter takes a jump towards the true value, but remains low. As additional observations accumulate, the $\Phi_{kf}(t)$ jumps varying amounts depending upon the particulars of the observations and their noise. Over the entire observation interval the energy remains low—*a systematic* error owing to the sparse observations and null space of $\mathbf{E}$. If the number of observations is greatly increased (not shown), the systematic error in the estimated energy vanishes. Here the forcing amplitude overall dominates the effects of the incorrect initial conditions. Uncertainty estimates for energy would once-again come from summations of correlated χ^2 variables of differing means. In the present case, the most important errors are the systematic ones visible as the offsets between the curves in Fig. 13.

This system can theoretically be over-determined by letting the number of observations at time t exceed the number of unknowns—should the null space of $\mathbf{E}(t)$ vanish. As expected, with 14 covarying observations, and 18 time-varying unknown $x_i(t)$, $\mathbf{E}(t)$ has a nullspace (is rank 12) and thus energy in the true field is missed even if the observations were perfect. As is conventional in inverse methods, the smaller eigenvalues and their corresponding eigenvectors are most susceptible to noise biases. The solution nullspace of this particular $\mathbf{E}(t)$ found from the solution eigenvectors of the singular value decomposition, $\mathbf{U}\Lambda\mathbf{V}^T = \mathbf{E}$. Solution resolution matrix at rank $K = 13$, $\mathbf{V}_K\mathbf{V}_K^T$, is shown in Fig. 14 where $\mathbf{V}_K$ contains the first K columns of $\mathbf{V}$. Thus the observations carry no information about modes (as ordered) 3,6,9,12,15,18. In

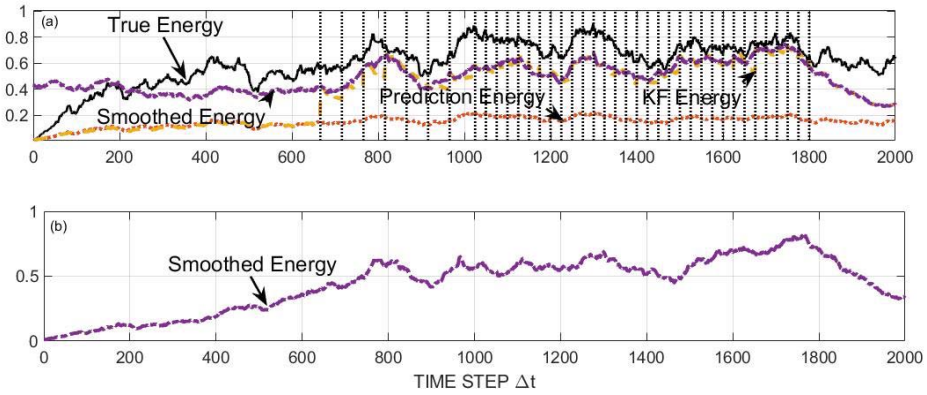

Figure 13: (a) The "energy", the sums $\Phi(t) = \sum_{nm} |\alpha_{nm}(t)|^2$, for the true and prediction models. In the prediction model, the initial conditions are 20% too large, and the forcing is 50% too small (but is otherwise identical to the true value). Time positions of the data, initially at every $50\Delta t$ and then at every 25th Δt, are shown. Prior to the data onset, the energy is that given by the prediction model. After the data interval, power is also from the prediction model, but starting with the final KF analysis estimate. Jumps in the KF power at observation times are visible, especially at the time of the first observation. The smoothed solution carries too much energy prior to the first observations as the system has no information about the growth of power before that time and the uncertainty assigned to the actual initial conditions is large. (b) The smoothed solution energy when initial conditions are set to be essentially perfect and showing the estimated reduced power towards the origin which does not occur when a finite uncertainty is assigned (as in (a)).

{rossby_pwr_al

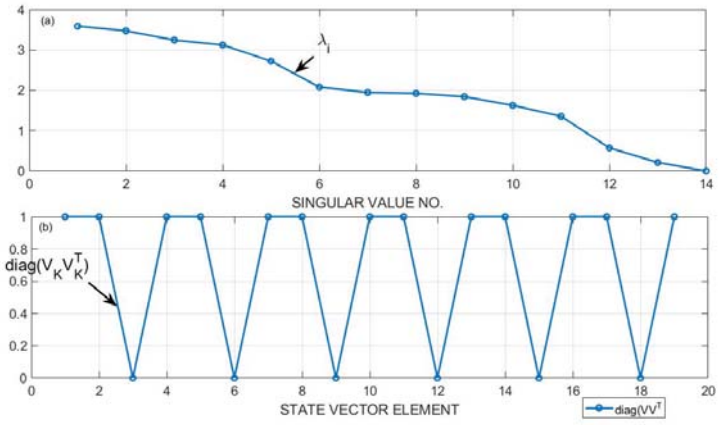

Figure 14: (a) First 14 singular vectors of $\mathbf{E}$. Rank is 13 with 14 observational positions. (b) Diagonal elements of the rank 13 solution resolution matrix (see W06), showing lack information for several of the modes. A value of 1 means that the mode is fully resolved by the observations. {rossby_svde1.

a real situation, if control over positioning of the observations was possible, this result could sensibly be modified and/or a strengthening of the weaker singular values could be achieved. Knowledge of the nullspace structure is very important in the interpretation of any of the results.

A more general discussion of nullspaces involves that of the weighted $\mathbf{P}(\tau,-)\mathbf{E}^T$ appearing in the Kalman gain. If $\mathbf{P}(\tau,-)^{1/2}$ is the Cholesky factor of $\mathbf{P}(\tau,-)$ (W06, P. 56), then $\mathbf{EP}(\tau,-)^{1/2}$ is the conventional column-weighting of $\mathbf{E}$ at time τ, and the resolution analysis would be applied to that combination. In the present system, $\mathbf{A}$ is diagonal, and thus it does not distribute information about any covariance amongst the elements $x_j(\tau)$ and which would be carried in $\mathbf{P}(\tau,-)$.

An important observational goal is determination of the north-south transport at each time-step from the velocity or stream function as,

$$WBC(t) = \psi(i=1, j_0, t) - \psi(i_0, j_0, t), \tag{44}$$ {wbctrans1}

at fixed latitude index j_0, as the stream-function difference between a longitude pair, i, i_0. From the boundary condition, $\psi(i=1, j_0, t) = 0$ identically. In the present context, five different values are relevant: (1) the true constant, invariant, value, (2) the true apparent value including the oscillatory mode noise, (3) the estimated value from the prediction model, (4) the estimate from the KF, (5) the estimate from the smoother. Fig. 15 displays the estimated transport from Eq. (44) for the correct value and from the KF estimate along with the standard error. Values here are dominated by the variability induced by the normal modes. Note that the result can depend sensitively on i_0, j_0 and the particular spatial structure of any given normal mode.

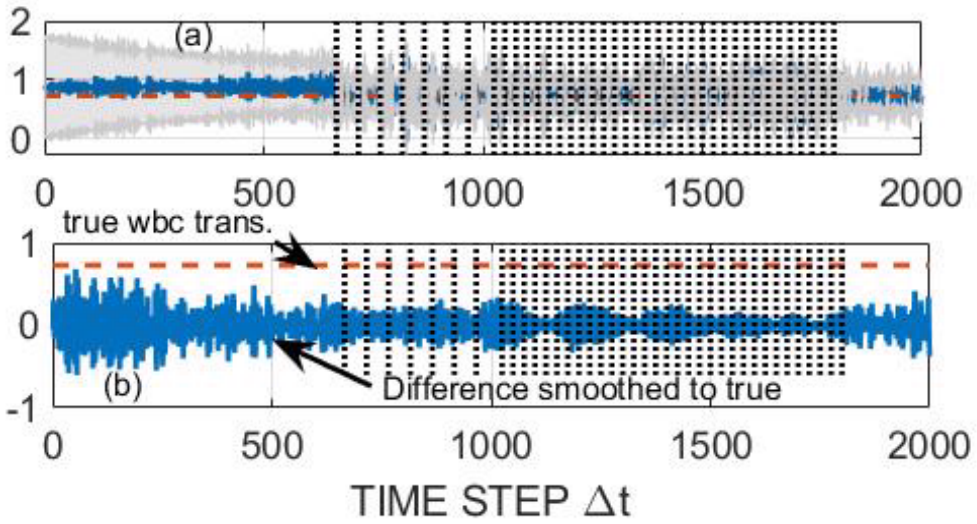

Figure 15: (a) Estimated western boundary current transport from the Kalman filter, and its standard error (gray field). (b) Same as (a) except for the smoothed solution and showing the difference between the true value and the estimated one.

{rossby_wbctra

In the KF (Fig. 15), observations move the WBC values closer to the truth, but do retain the normal mode noise. Prior to the first observation, the values are indistinguishable from zero. Within the observation interval, the estimates are indistinguishable from the true value but still have a wide uncertainty with time scales present both from the natural variability and the regular injection times of the data. Transport value uncertainties are derivable from the $\mathbf{P}$ of the state vector.

11.2 RTS Algorithm Results

Turning now to the RTS smoother, one sees in Fig. 13 that the energy, $\Phi_{smth}(t)$, in the smoothed solution is continuous (up to the usual time-stepping changes), but exceeds the true energy prior to the appearance of the first observation. The only information available to the smoother prior to the observational interval lies in the initial conditions, which were provided only with a very large uncertainty and the unknown $\mathbf{u}(t)$ in this interval also has a large variance. If the initial conditions are made near-perfect, the energy does decrease towards the origin as shown.

The smoother solution in the pre-data interval differs more widely from the true value than does the KF solution. That behavior is a consequence of the comparatively large uncertainty estimate assigned to the initial conditions. If the initial conditions are made near-perfect then (Fig.13), they are reproduced in the smoother solution and the reduced energy in that interval

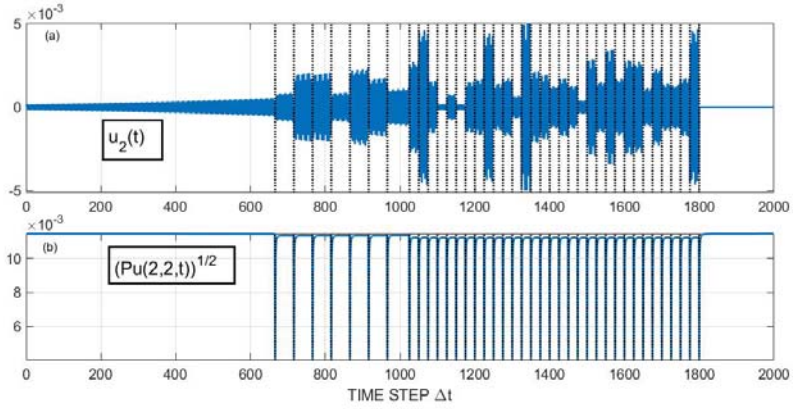

Figure 16: (a) One element, $u_2(t)$, of the control vector correction estimate and (b) its standard error through time, showing the drop to zero at the data time, and the rapid recovery to a higher value. {rossby_contro

is also the best estimate. An element through time of the control vector and its standard error are shown in Fig. 16. The complex result of the insertion of data is apparent. As with the KF, discussion of any systematic errors has to take place outside of the formalities leading to the smoothed solution.

Fig. 17 shows the behavior of the estimate of the WBC transport and its uncertainty when the smoothing algorithm is used with two different data densities. A test of the hypothesis that it was indistinguishable from constant would be based upon an analysis using the uncertainty (not shown here).

The very large uncertainty prior to the onset of data, even with use of a smoothing algorithm, is a central reason that the ECCO estimate (e.g., Fukumori, et al., 2018) is confined to the interval following 1992 when the data become far denser than before. Estimates prior to a dense data interval will depend greatly upon the time durations built into the system, which in the present case are limited by the longest normal mode period. The real ocean does include some very long memory (Wunsch and Heimbach, 2008), but the skill will depend directly on the specific physical variables of concern, and which in ECCO include the time-sensitive flow field.

Fig. 18 shows the norm of the operator $\mathbf{L}$ controlling the correction to earlier state estimates, along with the time dependence of one of the diagonal elements. The temporal structure of $\mathbf{L}$ in Eq. B1b depends directly upon the time constants embedded in $\mathbf{A}$, and the compositions of $\mathbf{P}(t), \mathbf{P}(t+\Delta t,-)$. In turn these latter are determined by any earlier information, including initial conditions, as well as the magnitudes and distributions of later forcing and data accuracies. Generalizations are not easy.

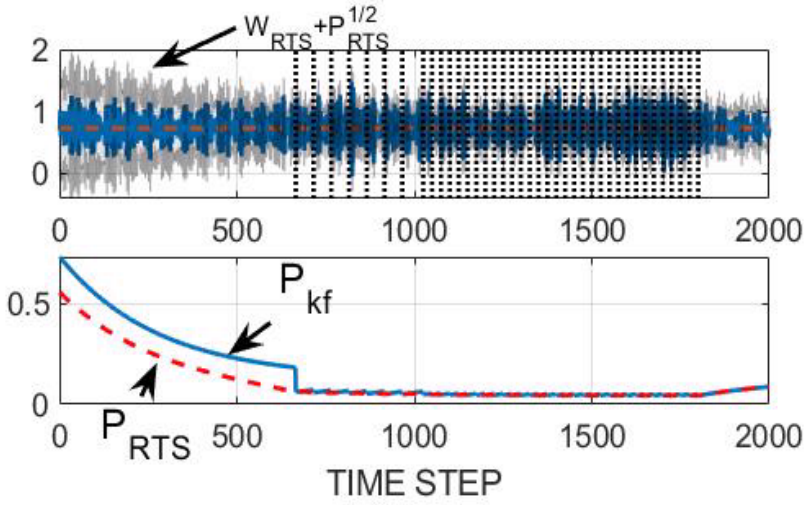

Figure 17: (a) Smoothed solution (blue line) estimate of the western boundary current transport and the true mean value along with the standard error of the KF estimate (gray lines). Data positions also shown. (b) Uncertainty in the WBC estimate for the KF and the smoothed values.

{rossby_wbctra

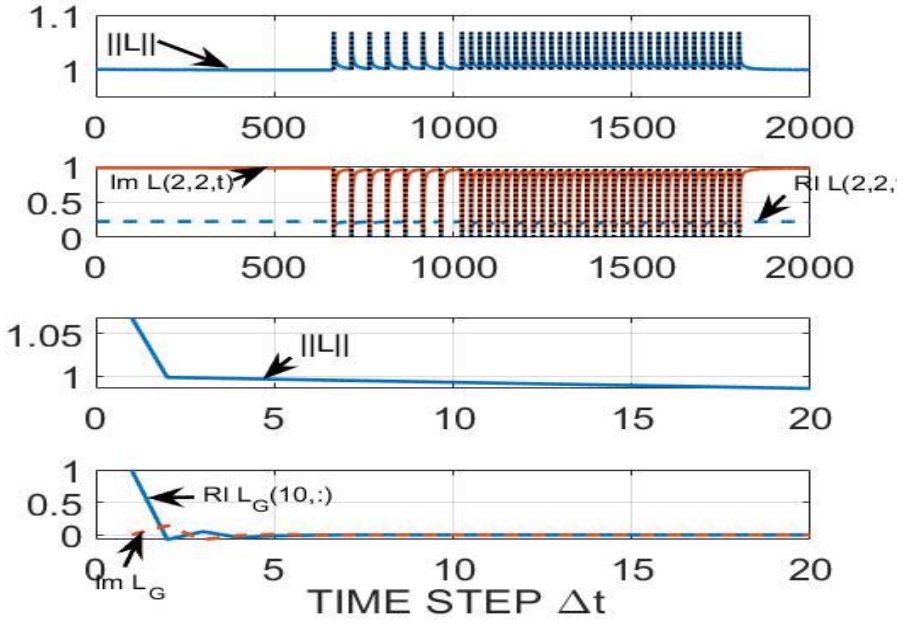

Figure 18: (a) Norm of the matrix **L** controlling the backwards in time state estimate. (b)

{rossby_lnorm_

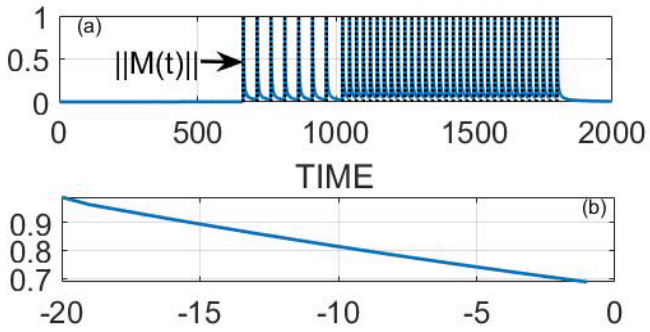

Figure 19: (a) Norm of the the gain matrix, $\mathbf{M}(t)$, through time (upper two panels) for the control value.(b) Norm of the products of $\mathbf{M}(t)$ for 20 backwards steps showing strong decrease from the prior observation.[??]

{rossby_mstore

The gain matrix $\mathbf{M}(t)$ for computation of the control vector is displayed in Fig. 19. Here the dependence is directly upon the a priori known $\mathbf{Q}(t)$, the data distributions, and the determinants of $\mathbf{P}(t+\Delta t,-)$. The limiting cases discussed above for the state vector also provide insights here.

11.3 Spectra

Computation of the spectral estimates of the various estimates of any state vector element or combination is straightforward and the $z-$transforms described in the text provide an analytic approach. What is not so straightforward is the interpretation of the result in this non-statistically stationary system. Care must be taken to account for the non-stationarity, but results are not further described here.

12 Discussion

The behavior of dynamical system invariants, be they fundamental ones such as energy or circulation or scalar inventory, or derived ones such as a current transport, in sequential estimation processes depends upon a number of parameters. These parameters include the time scales embedded in the dynamical system, the temporal distribution of the data relative to the embedded time-scales, the accuracies of initial conditions, boundary conditions, and data, as well as the accuracy of the governing time evolution model. In addition, the invariant estimates can depend directly upon the accuracies of the uncertainties, explicit or implicit, in all of the elements making up the estimation system. Because of their interplay, the only easy generalization is that the

user must check the accuracies of all of these elements, including the often difficult appearance of systematic errors in any of them. When feasible, a strong clue to the presence of systematic errors e.g., in energies, lies in determining the nullspace of the observation matrices coupled with the structure of the state evolution matrices, $\mathbf{A}$. Analogous examples have been computed e.g., for advection-diffusion systems (not shown, but see Marchal and Zhao, 2021) with analogous results concerning e.g., estimates of fixed total tracer inventories.

Physical insights into the system behavior are essential, as is an understanding of the structure of the imputed statistical relationships. As a considerable literature cited previously has made clear, the inference of trends in properties in the presence of time-evolving observation systems requires particular attention. At a minimum, one should test any such system against the behavior of a known result—e.g., treating a GCM as "truth" and then running the smoothing algorithms to test whether that truth is forthcoming.

Acknowledgement.

Supported from the NASA/UT Austin/JPL ECCO Projects. Work done at home during the Trump-Covid Apocalypse period.

13 Appendix B The Smoothing Problem

In the terminology of control theory and engineering, estimates using models and data and applying to finite time intervals are known as "smoothers." A variety of approaches exists (see e.g. Anderson and Moore, 1979; Goodwin and Sin, 1984). In the present context, it is the "fixed interval" smoother that is of most interest. Given the linear discrete time prediction model, and a set of noisy data distributed over times τ_i, find a weighted least-squares fit of the model to the data at the sampling times. In the prediction model, $\mathbf{u}(t)$ vanishes, as being unknown. The fitting can involve initial conditions, boundary conditions (contained in $\mathbf{q}, \mathbf{u}$), and the general forcing $\mathbf{q}$. Adjustments can be made to the model parameters themselves (elements of $\mathbf{A}$), but that renders the problem nonlinear, and although the subject has a large literature, it is ignored here. In any event, the result is one that satisfies the model over the entire time-domain along with whatever conservation requirements are implicit. $\mathbf{B}, \mathbf{\Gamma}$ have the configurations necessary to distribute the disturbances $\mathbf{q}, \mathbf{u}$ correctly over the state vector elements. Commonly, $\mathbf{B} = \mathbf{\Gamma}$. Direct, static, inversion of Eq. (4) for $\mathbf{x}(\tau_i, \mathbf{E})$ was described in above.

RTS Smoother

Consider the sequential algorithm usually known as the Rauch-Tung-Striebel (RTS) smoother, in which the assumption is made that the KF has been used, rigorously, over the finite interval $0 \leq t \leq T_{dur}$, producing the estimates denoted $\tilde{\mathbf{x}}(t,-), \tilde{\mathbf{x}}(t)$ with their corresponding uncertainty covariances $\mathbf{P}(t,-), \mathbf{P}(t)$. At this stage, no further discussion of the data occurs: all information contained in the observations has been exploited by the KF and is encompassed in $\tilde{\mathbf{x}}(t)$ and its uncertainty $\mathbf{P}(t)$. What has not been exploited in an estimate $\tilde{\mathbf{x}}(t), \mathbf{P}(t)$, is any information contained in data that were obtained *afterwards*, $t + m\Delta t > t$, *but that information is present in any later estimates* $\tilde{\mathbf{x}}(t + m\Delta t), \mathbf{P}(t + m\Delta t)$.

The logic of the RTS smoother is to compare the change that took place between $\tilde{\mathbf{x}}(t,-)$ and $\tilde{\mathbf{x}}(t)$, and its uncertainty, to estimate the unknown elements in $\mathbf{q}(t)$, (called $\mathbf{u}(t)$) and to improve the *preceding* estimate $\tilde{\mathbf{x}}(t - \Delta t, -)$ and its uncertainty. If done rigorously—up to the various assumptions—the result is a system in which changes in the physical invariants can be properly attributed to specific, estimated, forcing/sources/sinks, etc. over the entire time interval being considered.

The resulting RTS algorithm is more complex appearing than is the KF, because all of the later estimates have a finite correlation with the previous ones and they cannot be simply combined without first removing that correlation. (The scalar state vector case is readily analyzed without any matrix/vector algebra and is written out in Appendix C.) As described in the numerous textbooks, the RTS algorithm is, {rts1}

$$\tilde{\mathbf{x}}(t,+) = \tilde{\mathbf{x}}(t) + \mathbf{L}(t+\Delta t)\,[\tilde{\mathbf{x}}(t+\Delta t,+) - \tilde{\mathbf{x}}(t+\Delta t,-)]\,, \tag{B1a} \{\texttt{rts1a}\}$$

$$\mathbf{L}(t+\Delta t) = \mathbf{P}(t)\mathbf{A}(t)^T\,\mathbf{P}(t+\Delta t,-)^{-1}, \tag{B1b} \{\texttt{rts1b}\}$$

{rts2}

$$\tilde{\mathbf{u}}(t,+) = \mathbf{M}(t+\Delta t)\,[\tilde{\mathbf{x}}(t+\Delta t,+) - \tilde{\mathbf{x}}(t+\Delta t,-)]\,, \tag{B2a} \{\texttt{rts2a}\}$$

$$\mathbf{M}(t+\Delta t) = \mathbf{Q}(t)\mathbf{\Gamma}(t)^T\mathbf{P}(t+\Delta t,-)^{-1}, \tag{B2b} \{\texttt{rts2b}\}$$

{PQ}

$$\mathbf{P}(t,+) = \mathbf{P}(t) + \mathbf{L}(t+\Delta t)\,[\mathbf{P}(t+\Delta t,+) - \mathbf{P}(t+\Delta t,-)]\,\mathbf{L}(t+\Delta t)^T, \tag{B3a} \{\texttt{Ptplusa}\}$$

$$\mathbf{Q}(t,+) = \mathbf{Q}(t) + \mathbf{M}(t+\Delta t)\,[\mathbf{P}(t+\Delta t,+) - \mathbf{P}(t+\Delta t,-)]\,\mathbf{M}(t+\Delta t)^T, \tag{B3b} \{\texttt{Ptpb}\}$$

involving the estimate at a formally future time, $t + \Delta t$. (As always, in the forward, prediction, the unknown $\mathbf{u}(t) = 0$.) The + in the argument is used to label the estimates of these variables as having employed the formally *future* data.

Algorithmically, these equations are run "backwards" in time from $t = T_{dur}$ using the terminal time estimates $\tilde{\mathbf{x}}\left(T_{dur}\right), \mathbf{P}\left(t_{dur}\right)$ found from the KF as the starting values. The main point here is that one obtains new estimates $\tilde{\mathbf{x}}(t,+), \mathbf{P}\left(t,+\right)$ that use the information about the formally future data, as well as estimates of the changes required in the forcing/boundary conditions etc., $\mathbf{u}(t,+)$, and their uncertainty $\mathbf{Q}(t,+)$. The result is a system, $\tilde{\mathbf{x}}(t,+), \mathbf{u}(t,+)$ that now satisfies the original prediction equation including its implicit or explicit invariants, but with modified values of the initial and boundary conditions, such that the data are also consistent within their error bars. As with the discussion of the various nullspaces of $\mathbf{E}$, $\mathbf{Q}(t)\mathbf{\Gamma}(t)^T$ will determine the extent to which elements of $\tilde{\mathbf{u}}(t,+)$ can be resolved from the observations.

Limiting Cases

The RTS smoother algorithm is not very intuitive. Consider two limiting cases. First, suppose that at time t, it is known that no forcing has occurred, $\mathbf{Q}\left(t\right) = \mathbf{0}$ and then $\tilde{\mathbf{u}}\left(t,+\right) = \mathbf{0}$. Eq. (B1a) produces (assuming the inverses exist),

$$\begin{aligned}
\tilde{\mathbf{x}}(t,+) - \tilde{\mathbf{x}}(t) &= \mathbf{P}(t)\mathbf{A}(t)^T \left(\mathbf{A}\left(t\right)\mathbf{P}\left(t\right)\mathbf{A}\left(t\right)\right)^{-1}\left[\tilde{\mathbf{x}}(t+\Delta t,+) - \tilde{\mathbf{x}}(t+\Delta t,-)\right] \\
&= \mathbf{P}(t)\mathbf{A}(t)^T \left(\mathbf{A}\left(t\right)^{-T}\mathbf{P}\left(t\right)^{-1}\mathbf{A}\left(t\right)^{-1}\right)\left[\tilde{\mathbf{x}}(t+\Delta t,+) - \tilde{\mathbf{x}}(t+\Delta t,-)\right] \\
&= \mathbf{A}\left(t\right)^{-1}\left[\tilde{\mathbf{x}}(t+\Delta t,+) - \tilde{\mathbf{x}}(t+\Delta t,-)\right],
\end{aligned} \tag{B4}$$

that is, the backwards in time correction is simply the model run backwards in time on the discrepancy seen at $t + \Delta t$.

Now consider the opposite limit, in which $\tilde{\mathbf{x}}(t)$ is known perfectly, so that $\mathbf{P}\left(t\right) = \mathbf{0}$. Then $\mathbf{P}\left(t+\Delta t,-\right) = \mathbf{\Gamma}\mathbf{Q}\left(t\right)\mathbf{\Gamma}^T$, owing to the unknown forcing only. Then, $\mathbf{L}(t+\Delta t) = 0$, and the previous perfect state estimate remains unchanged, $\tilde{\mathbf{x}}(t,+) = \tilde{\mathbf{x}}(t)$. Also,

$$\begin{aligned}
\mathbf{M}(t+\Delta t) &= \mathbf{Q}(t)\mathbf{\Gamma}(t)\left[\mathbf{\Gamma}(\mathbf{t})\mathbf{Q}\left(t\right)\mathbf{\Gamma}(t)^T\right]^{-1} \\
&= \mathbf{Q}(t)\mathbf{\Gamma}(t)^T\mathbf{\Gamma}(t)^{-T}\mathbf{Q}\left(t\right)^{-1}\mathbf{\Gamma}(t)^{-1} = \mathbf{\Gamma}(t)^{-1}
\end{aligned} \tag{B5}$$

$$\tilde{\mathbf{u}}(t,+) = \mathbf{\Gamma}\left(t\right)^{-1}\left[\tilde{\mathbf{x}}(t+\Delta t,+) - \tilde{\mathbf{x}}(t+\Delta t,-)\right], \tag{B6}$$

simply an estimate of what the disturbance was. Generally, $\mathbf{\Gamma}^{-1}$ does not exist ($\mathbf{\Gamma}$ will almost never be a full-rank square matrix), and a generalized inverse could be used—leaving a null-space in $\tilde{\mathbf{u}}(t,+)$ as part of its uncertainty. Between these two limits, the algorithm partitions changes in the earlier state vector and in the control according to their relative covariances.

Appendix C Scalar Systems

The algebraic statement of the smoother is not easy to penetrate. Consider an even simpler system–that of a scalar obeying a time evolution equation, the "prediction equation" in the above terminology is,

$$x\left(t+\Delta t\right)=ax\left(t\right)+bq\left(t\right)+\Gamma\left(t\right)u\left(t\right) \tag{C1}$$ {c1}

where $|a|<1$ is a constant, and $q\left(t\right)$ is a known forcing process. $\Gamma\left(t\right)u\left(t\right)$ has zero-mean and variance $Q\left(t\right)$, perhaps constant in time, and represents any unknown element in $q\left(t\right)$. Q is used as $u\left(t\right)$ represents the uncertainty in q. b,Γ are known scale factors and might as well be taken as 1, but are useful markers. Let there be observations of $x\left(\tau\right)$,

$$y\left(\tau\right)=Ex\left(\tau\right)+\varepsilon\left(\tau\right) \tag{C2}$$ {c2}

where the observation noise, $\varepsilon\left(t\right)$, is another zero-mean white noise process of variance, R. The system begins at $t=0$, with an initial condition $\tilde{x}\left(0\right)$, with a known uncertainty, $P\left(0\right)=\left(\tilde{x}\left(0\right)-x\left(0\right)\right)^{2}$. No null space of E exists

The Kalman Filter

Prediction is made using Eq. (C1) with the unknown $u\left(t\right)$ set to zero and the estimated initial condition. Then

$$\tilde{x}\left(t+\Delta t,-\right)=a\tilde{x}\left(t\right)+bq\left(t\right). \tag{C3}$$ {c3}

At the previous time-step, the uncertainty, $P\left(t\right)=\left(\tilde{x}\left(t\right)-x\left(t\right)\right)^{2}$, is known, and then the uncertainty of the prediction is,

$$P\left(t+\Delta t,-\right)=a^{2}P\left(t\right)+\Gamma^{2}Q\left(t\right) \tag{C4}$$ {c4}

with as before, the minus sign indicating that no data at time $t+\Delta t$ have been used. *If no data are available*, $\tilde{x}\left(t+\Delta t\right)=\tilde{x}\left(t\right)$, and its uncertainty is $P\left(t+\Delta t\right)=P\left(t+\Delta t,-\right)$ with Eq. (C4) becoming,

$$P\left(t+\Delta t\right)=a^{2}P\left(t\right)+\Gamma^{2}Q(t), \tag{C5}$$ {c5}

a simple difference equation which can be solved beginning at $t=0$.

If no data at all are available, taking the $z-$transform, $z=\exp\left(-2\pi is\Delta t\right)$, and denoting the result with a circumflex,

$$\hat{P}\left(z\right)/z=a^{2}\hat{P}\left(z\right)+\Gamma^{2}\hat{Q}(z) \tag{C6}$$ {c6}

and

$$\hat{P}\left(z\right)=\frac{z\hat{Q}\left(z\right)}{1-za^{2}}=\hat{Q}\left(z\right)z\left(1+za^{2}+z^{2}a^{4}+...\right) \tag{C7}$$ {c7}

If Q is a constant, $\hat{Q}(z) = Q_0\left(1 + z + z^2 + ...\right)$,

$$\begin{aligned}\hat{P}(z) &= Q_0\left(z + z^2 + z3 + ...\right)\left(1 + a^2 z + a^4 z + a^6 z^3 + ...\right) \\ &= \frac{zQ_0}{\left(1 - za^2\right)(1 - z)}\end{aligned} \tag{C8}$$ {c8}

and which will not converge on $|z| = 1$; the pole at $z = 1$ arises from the accumulating influence of the constant Q. One might assume a vanishingly small decay constant, $\delta \to 0$, so that $Q(t) = (1 - t\delta) Q_0$ and then,

$$\hat{P}(z) = \frac{z\Gamma^2 Q_0}{\left(1 - za^2\right)\left(1 - (1 - \delta) z\right)}, \tag{C9}$$ {c9}

is now interpretable as a Fourier transform on $|z| = 1$.

If data are available at time τ,

$$\tilde{x}(\tau) = \tilde{x}(\tau, -) + \frac{P(\tau, -) E}{[E^2 P(\tau, -) + R]}(y(\tau) - E\tilde{x}(\tau, -)) \tag{C10}$$ {c10}

where the difference, $y(\tau) - E\tilde{x}(\tau, -)$ includes both the observational noise, and the discrepancies in the predicted state from the true value. Evidently, any mis-specification of a, E, Q or $P(0)$ will lead to an error in the estimate, and in its uncertainty. With $a < 1$, the influence of initial condition, $\tilde{x}(0)$, will fade with time. In the limit of zero observational noise,

$$\tilde{x}(\tau) = \tilde{x}(\tau, -) + \frac{P(\tau, -) E}{E^2 P(\tau, -)}(y(\tau) - E\tilde{x}(\tau, -)) = y(\tau)/E,$$

as one would expect. In the opposite limit of very large noise, no change is made in $\tilde{x}(\tau, -)$.

The uncertainty following employment of the observation at $t = \tau$ is

$$P(\tau) = P(\tau, -)\left(1 - \frac{P(\tau, -) E^2}{E^2 P(\tau, -) + R}\right) \leq P(\tau, -)$$

that is, the data reduces the uncertainty. Should $R \to 0$, $P(\tau)$ vanishes but would become finite again at the next predicted time-step. If $R \to \infty$, $P(\tau) = P(\tau, -)$.

Smoother

Now assuming that the KF has been run out to a duration $0 \leq t \leq T_{dur}$, the Rauch-Tung-Striebel (RTS) algorithm can be used to improve the estimates using observations that were formally future to times τ in the KF. Let any such new estimate be denoted $\tilde{x}(t, +)$, with a new uncertainty $P(t, +)$. Then for this scalar system,

$$\tilde{x}(t, +) = \tilde{x}(t) + \frac{P(t) a}{P(t + \Delta t, -)}\left[\tilde{x}(t + \Delta t, +) - \tilde{x}(t + \Delta t, -)\right] \tag{C11}$$

so that if there were no data *future* to $t+\Delta t$, $\tilde{x}(t+\Delta t,+)=\tilde{x}(t+\Delta t,-)$, and no change is made in the previous value, $\tilde{x}(t)$. If, previously, $\tilde{x}(t)$,were know perfectly, $P(t)=0$, and again no change is made.

Supposing $\tilde{x}(t+\Delta t,+)$ were perfect e.g., from a perfect observation at that time, $\tilde{x}(t)$ is not simply replaced by the model run backwards, because the change is appropriately partitioned between $\tilde{x}(t,+)$ and $\tilde{u}(t,+)$ .The estimated unknown control variable in that interval is,

$$\tilde{u}(t,+)=\frac{Q(t)\Gamma(t)}{P(t+\Delta t,-)}\left[\tilde{x}(t+\Delta t,+)-\tilde{x}(t+\Delta t,-)\right] \tag{C12}$$

If $\tilde{x}(t+\Delta t,+)$ is perfect, $\tilde{u}(t)$ is directly proportional to the difference between the predicted $\tilde{x}(t+\Delta t,-)$ and the true value, but not equal to it because some of the change is allotted to $\tilde{x}(t,+)$ .Similar constructs can be inferred for the various uncertainties. Should $Q=0$, $\tilde{u}(t,+)=0$, and with $P(t+\Delta t,-)=a^2P(t,)$, then $\tilde{x}(t,+)=\tilde{x}(t)=1/a\left[\tilde{x}(t+\Delta t,+)-\tilde{x}(\tau+\Delta t,-)\right]$.

Appendix D. Direct Least-Squares Solution

That sequential estimation requires knowledge of the uncertainties at each stage leads to consideration of *non-sequential* methods, whose great advantage is avoidance of that major computational burden. Their chief weakness, however, is the corresponding absence of knowledge of the uncertainties. Nonetheless, it is useful to understand how those methods work, particularly as systems such as ECCO (see e.g., Fukumori et al., 2018, 2019) rely upon these non-sequential approaches. Although the methodology has a number of opaque labels (e.g., "4DVAR", or "adjoint"), algorithmically it is simply a form of recursive weighted least-squares with Lagrange multipliers (e.g., W06 and references there). One begins, as in all least-squares problems, with the statement of an objective function to be minimized, for example,

$$J_1=\sum_{t=1}^{N_T}\left(\mathbf{y}(t)-\mathbf{E}(t)\mathbf{x}(t)\right)^T\mathbf{R}(t)^{-1}\left(\mathbf{y}(t)-\mathbf{E}(t)\mathbf{x}(t)\right)+ \tag{D1}$$
$$\left(\mathbf{x}(0)-\mathbf{x}_0\right)^T\mathbf{P}(0)^{-1}\left(\mathbf{x}(0)-\mathbf{x}_0\right)+\sum_{t=1}^{N_T-1}\mathbf{u}(t)^T\mathbf{Q}(t)^{-1}\mathbf{u}(t)$$

where the first term is a conventional weighted misfit of the state estimate to the data, the second term is the misfit to the initial conditions (which could be included in the "data"), and the third term attempts to minimize the control, $\mathbf{u}(t)$, from its initial estimate, weighted by its prior uncertainty matrix. The minimization is subject to the model evolution being correct, and that is appended using Lagrange multipliers, $\boldsymbol{\mu}(t)$, so that the final objective function is,

$$J=J_1-2\boldsymbol{\mu}(t)^T\left[\mathbf{x}(t+\Delta t)-\mathbf{A}\mathbf{x}(t)-\mathbf{B}\mathbf{q}(t)-\Gamma\mathbf{u}(t)\right], \tag{D2}$$

whose stationary value is to be found. Because an error term, $\Gamma \mathbf{u}(t)$, appears in the appended model, this constraint is a "soft" one. (Again, $\mathbf{A}, \mathbf{B}$, $\mathbf{\Gamma}$ can be time-dependent, and the model can be non-linear.) Setting all the partial derivatives in Eq. (D2) with respect to $\mathbf{x}(t)$, $t = 0, ..., T, \mathbf{u}(t), t = 0, T - \Delta t$, and $\boldsymbol{\mu}(t), t = 0, T - 1$ to zero, one obtains conventional normal equations. In practice, the appended model is nonlinear.

This resulting system has an equal number of equations and unknowns and in principle can be solved like any other set of linear simultaneous equations. In practice, the dimension is so large, that a great deal of attention has been paid to solving it recursively (Heimbach et al., 2009). Without going into those details, note that *the resulting solution is identical to that found from the smoothing algorithm*, but without the burden of finding the uncertainty matrices. As discussed in the various references, knowledge of $\boldsymbol{\mu}(t)$ permits a highly efficient calculation of sensitivities to various elements, although not a formal statistical uncertainty.

In the normal equations resulting from taking the derivatives in Eq. (D1, and see W06), the transposed $\mathbf{A}$ matrix (the adjoint matrix) is very important. Claerbout (2014, Ch. 1) gives a number of useful intuitive physical interpretations of algebraic adjoints. In the same way that nonlinear systems lead to successive linearizations through the extended Kalman filter and corresponding smoothers, the least-squares system can be readily solved by iteration (Heimbach et al., 2009). (These non-linear extensions make assumptions about the degree and type of nonlinearity, but that discussion is outside the present scope.)

References

Anderson, B. D. O., and J. B. Moore, 1979: Optimal Filtering. Prentice-Hall, Englewood Cliffs, N. J., 357 pp.

Bengtsson, L., S. Hagemann, and K. I. Hodges, 2004: Can climate trends be calculated from reanalysis data? J. Geophys. Res., D11, Art No. D11111.

Bengtsson, L., and Coauthors, 2007: The need for a dynamical climate reanalysis. Bulletin of the American Meteorological Society, 88, 495-501.

Boers, N., 2021: Observation-based early-warning signals for a collapse of the Atlantic Meridional Overturning Circulation. Nature Clim. Change, 11, 680-688.

Brogan, W., 1991: Modern Control Theory. Third Ed. Prentice-Hall, Englewood Cliffs, NJ.

Bromwich, D. H., and R. L. Fogt, 2004: Strong trends in the skill of the ERA-40 and NCEP-NCAR reanalyses in the high and midlatitudes of the southern hemisphere, 1958-2001. Journal of Climate, 17, 4603-4619.

Brown, R. G., and P. Y. C. Hwang, 1997: Introduction to Random Signal Analysis and Applied Kalman Filtering: with MATLAB Exercises and Solutions, 3rd Ed. Wiley, New York, 484347pp pp.

Bucy, R. S., and P. D. Joseph, 1968: Filtering for Stochastic Processes with Applications to Guidance. Wiley, New York, 195 pp pp.

Carton, J. A., and B. S. Giese, 2008: A reanalysis of ocean climate using Simple Ocean Data Assimilation (SODA). Monthly Weather Review, 136, 2999-3017.

Davies, R. B., 1980: Algorithm AS 155: The Distribution of a Linear Combination of χ^2 Random Variables. Journal of the Royal Statistical Society. Series C (Applied Statistics), 29, 323-333.

Evensen, G., 2009: Data Assimilation: The Ensemble Kalman Filter. Springer Verlag.

Farebrother, R. W., 1984: Remark AS R53: A Remark on Algorithms AS 106, AS 153 and AS 155: The Distribution of a Linear Combination of χ^2 Random Variables. Journal of the Royal Statistical Society. Series C (Applied Statistics), 33, 366-369.

Fukumori, I., P. Heimbach, R. M. Ponte, and C. Wunsch, 2018: A dynamically-consistent ocean climatology and its temporal variations. Bull. Am. Met. Soc., Oct., 2107-2127.

Fukumori, I., O. Wang, I. Fenty, G. Forget, P. Heimbach, and R. M. Ponte, 2019: ECCO Version 4 Release 4, https://ecco.jpl.nasa.gov/drive/files/Version4/Release4/doc/v4r4_synopsis.pdf.

Gaspar, P., and C. Wunsch, 1989: Estimates from altimeter data of barotropic Rossby waves in the northwestern Atlantic Ocean. J. Phys. Oc., 19, 1821-1844.

Goldstein, H., 1980: Classical Mechanics, 2nd ed. Addison-Wesley, Reading, Mass, 672 pp pp.

Goodwin, G. C., and K. S. Sin, 1984: Adaptive Filtering Prediction and Control. Prentice-Hall,

Englewood Cliffs, N. J., 540 pp.

Hairer, E., C. Lubich, and G. Wanner, 2006: Geometric Numerical Integration: Structure-preserving Algorithms for Ordinary Differential Equations. Springer.

Hill, D. J., and P. J. Moylan, 1980: Dissipative dynamical-systems—basic input-output and state properties. Journal of the Franklin Institute-Engineering and Applied Mathematics, 309, 327-357.

Hu, S., J. Sprintall, C. Guan, M. J. McPhaden, F. Wang, D. M. Hu, and W. Cai, 2020: Deep-reaching acceleration of global mean ocean circulation over the past two decades. Science Advances, 6, eaxx7727.

Imhof, J. P., 1961: Computing the distribution of quadratic forms in normal variables. Biometrika, 48, 419?426.

Kalman, R. E., 1960: A new approach to linear filtering and prediction problems. J. Basic Eng., 82, 35-45.

Kim, S. J., K. Koh, S. Boyd, and D. Gorinevsky, 2009: l(1) Trend Filtering. Siam Review, 51, 339-360.

Konstantinov, M. M., P. H. Petkov, and N. D. Christov, 1993: Perturbation analysis of the discrete Riccati equation. Kybernetica, 29, 18-29.

LaCasce, J. H., 2002: On turbulence and normal modes in a basin. Journal of Marine Research, 60, 431-460.

Lauritzen, S. L., 1981: Time series analysis in 1880. A discussion of contributions made by T.N. Thiele. International Statistical Review, 49, 319?331. doi:310.2307/1402616. JSTOR 1402616.

Levinson, N., 1947: A heuristic exposition of Wiener's mathematical theory of prediction and filtering. J. Math. Phys., 25, 261-278 Reprinted as Appendix C of Wiener (1949).

Liebelt, P. B., 1967: An Introduction to Optimal Estimation. Addison-Wesley, Reading, Mass., 273pp. pp.

Longuet-Higgins, M. S., 1964: Planetary waves on a rotating sphere. Proc. Roy. Soc., A., 279, 446-473.

Luther, D. S., 1982: Evidence of a 4-6 day barotropic planetary oscillation of the Pacific Ocean. J. Phys. Oc., 12, 644-657.

McCuskey, S. W., 1959: An Introduction to Advanced Dynamics. Addison-Wesley Pub. Co..

Morse, P. M., and H. Feshbach, 1953: Methods of Theoretical Physics, 2 vols. McGraw-Hill, New York, 1978pp. pp.

Pedlosky, J., 1965: A study of time dependent ocean circulation. Journal of the Atmospheric Sciences, 22, 267-&.

Pedlosky, J., 2003: Waves in the Ocean and Atmosphere: Introduction to Wave Dynamics.

876 Springer, Berlin, 250pp. pp.
877 Piantadosi, S. T., 2018: One parameter is always enough. AIP Advances, 095118.
878 Pilo, G. S., P. R. Oke, R. Coleman, T. Rykova, and K. Ridgway, 2018: Impact of data assimi-
879 lation on vertical velocities in an eddy resolving ocean model. Ocean Modelling, 131, 71-85.
880 Ponte, R. M., 1997: Nonequilibrium response of the global ocean to the 5-Day Rossby? Haur-
881 witz wave in atmospheric surface pressure. Journal of Physical Oceanography, 27, 2158-2168.
882 Schreier, P. J., and L. L. Scharf, 2010: Statistical Signal Processing of Complex-Valued Data :
883 The Theory of Improper and Noncircular Signals. Cambridge University Press, xix, 309 p. pp.
884 Sewell, M. J., 1987: Maximum and Minimum Principles. A Unified Approach with Applications.
885 Cambridge Un. Press, Cambridge, 468pp pp.
886 Sheil, J., and I. O'Muircheartaigh, 1977: Algorithm AS 106: The Distribution of Non-Negative
887 Quadratic Forms in Normal Variables. Journal of the Royal Statistical Society. Series C (Ap-
888 plied Statistics), 26, 92-98.
889 Stengel, R. F., 1986: Stochastic Optimal Control. Wiley-Interscience, N. Y., 638 pp pp.
890 Stommel, H., 1948: The westward intensification of wind-driven ocean currents. Trans. Am.
891 Geophys. Un., 29, 202-206.
892 Storto, A., and Coauthors, 2019: Ocean reanalyses: Recent advances and unsolved challenges.
893 Frontiers in Marine Science, 6.
894 Strang, G., 2007: Computational Science and Engineering Wellesley-Cambridge Press.
895 Tan, Z. Q., Y. C. Soh, and L. H. Xie, 1999: Dissipative control for linear discrete-time systems.
896 Automatica, 35, 1557-1564.
897 Thorne, P. W., and R. S. Vose, 2010: Reanalyses suitable for characterizing long-term trends.
898 Are they really achievable? Bulletin of the American Meteorological Society, 91, 353-361.
899 Woodworth, P. L., S. A. Windle„ and J. M. Vassie, 1995: Departures from the local inverse
900 barometer model at periods of 5 days in the central South Atlantic. J. Geophys. Res., 100,
901 18,281-218,290.
902 Wunsch, C., 2006: Discrete Inverse and State Estimation Problems: With Geophysical Fluid
903 Applications. Cambridge University Press, xi, 371 pp.
904 Wunsch, C., 2020: Is the ocean circulation speeding up? Ocean surface trends. J. Phys. Oc. ,
905 50, 3205-3217.
906 Wunsch, C., and P. Heimbach, 2008: How long to ocean tracer and proxy equilibrium? Quat.
907 Sci. Rev., 27., doi:10.1016/j.quascirev.2008.1001.1006, 1639-1653.
908 Zhou, L. M., Y. Lin, Y. Wei, and S. Qiao, 2009: Perturbation analysis and condition numbers
909 of symmetric algebraic Riccati equations. Automatica, 45, 1005-1011.